

GAS - LIQUID MASS TRANSFER  
IN AN AGITATED VESSEL:  
AIR - WATER SYSTEM

By

ÖNER HORTAÇSU

Bachelor of Science

Robert College

İstanbul, Turkey

1963

Submitted to the faculty of the Graduate School of  
the Oklahoma State University  
in partial fulfillment of the requirements  
for the degree of  
MASTER OF SCIENCE  
August, 1965

Tthesis  
1965  
H 8219  
cop. 2

OKLAHOMA  
STATE UNIVERSITY  
LIBRARY

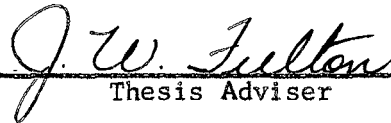
DEC 8 1965


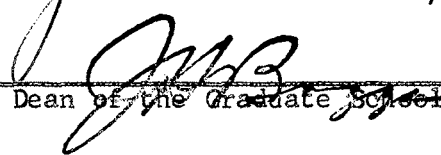
GAS - LIQUID MASS TRANSFER

IN AN AGITATED VESSEL:

AIR - WATER SYSTEM

Thesis Approved:

  
\_\_\_\_\_  
Thesis Adviser

  
\_\_\_\_\_  
  
\_\_\_\_\_  
Dean of the Graduate School

593503

## PREFACE

This work includes the correlation of the mass transfer coefficient-interfacial area product  $k_L a$  as a function of the agitation rate, superficial gas velocity, and temperature in an agitated gas-liquid contactor for the transfer of oxygen from air bubbles to water. The effect of solid particles on the mass transfer with mechanical agitation was also studied.

I am especially thankful to Dr. James W. Fulton, my research adviser, for his advice and counsel, and also to Dr. Samuel Sideman, and to Dr. John B. West for their enlightening advice and help during this study. I am also thankful to Dr. Robert N. Maddox, Professor Wayne C. Edmister, Dr. John J. Erbar, Dr. Kenneth J. Bell, and to Dr. Kwang Chu Chao for unselfishly contributing their time and efforts during my graduate work. I would also like to express my gratitude to the members of the faculty and staff of Robert College, and especially to Dr. Turgut Noyan, and to Dr. Carlo O. Ml̄oh, both of Robert College, for their advice, help, teaching and guidance during my undergraduate work, and for their continued interest in my graduate work.

I am grateful to Anadolu Tasfiyehanesi Anonim Şirketi, (A.T.A.Ş.), of Mersin, Turkey, and to the Oklahoma State University School of Chemical Engineering for financing my graduate work.

I would also like to thank all my friends, especially to Dr. James L. Webster, who have showed interest and graciously helped me all through

my work, and to Mr. E. R. Laminack for his continued interest and support. Thanks are also due to Mr. Eugene E. McCroskey for his help in securing and assembling the experimental apparatus.

Above all, I would like to express my eternal indebtedness to my parents, brother, and sister in Turkey for their support, interest, encouragement, patience, and sacrifices all through my life.

## TABLE OF CONTENTS

Chapter	Page
I. INTRODUCTION. . . . .	1
II. A SURVEY OF THE LITERATURE. . . . .	4
Two Film Theory. . . . .	5
Penetration (Surface Renewal) Theory . . . . .	6
Boundary Layer Theory. . . . .	8
Kinetic Theory of Gas Absorption . . . . .	9
Bubble Characteristics . . . . .	9
Stages of Bubble Life. . . . .	12
Nature of the Transfer Coefficient . . . . .	13
Studies on Oxygen Absorption by Water from Bubbles in Agitated Gas-Liquid Contactors . . . . .	16
III. EXPERIMENTAL. . . . .	27
Apparatus. . . . .	27
Agitated Vessel . . . . .	27
Constant Temperature Bath . . . . .	28
Dissolved Oxygen Analyzer . . . . .	28
Other Auxillary Equipment . . . . .	29
Materials. . . . .	32
Experimental Procedure . . . . .	32
Adjustment of the Constant Temperature Bath . . . . .	33
Driving the Dissolved Oxygen Out of the Water . . . . .	33
Adjustment of Stirrer Speed . . . . .	34
Calibration of the Flowmeter. . . . .	35
Timing the Aeration . . . . .	36
Calibration of the Dissolved Oxygen Analyzer. . . . .	38
Dissolved Oxygen Concentration Measurements . . . . .	39
Preparation of the Plastic Particles. . . . .	40
Experiments With Particles in the Agitated Vessel . . . . .	40
Approximate Measurement of the Bubble Size. . . . .	41
Effect of Surface Aeration. . . . .	41
IV. DISCUSSION OF RESULTS . . . . .	42
$k_L a$ as a Function of $N^3 D^2$ , $N_{Re}$ , and $N$ . . . . .	42
$k_L a$ as a Function of $V_s$ . . . . .	52
$k_L a$ as a Function of $T$ . . . . .	52
Transition Point in the $\log k_L a$ Versus $\log N^3 D^2$ Plots . . . . .	54
Dependence of $k_L a$ on $N^3 D^2$ , and on $V_s$ in the Absence of Mechanical Agitation. . . . .	55

$k_L a$ as a Function of $N^3 D^2$ , $V_S$ , and $T$ . . . . .	58
Sources of Experimental Error. . . . .	60
V. CONCLUSIONS AND RECOMMENDATIONS . . . . .	62
A SELECTED BIBLIOGRAPHY. . . . .	65
APPENDICES . . . . .	69
A. Dissolved Oxygen Analyzer Calibration Chart . . . . .	70
B. Chart and Sample Calculations for $k_L a$ Determination . . . . .	71
C. Reproducibility of the $k_L a$ 's, and Consistency of the Dissolved Oxygen Analyzer Readings. . . . .	73
D. Experimental $k_L a$ Values . . . . .	76
E. Bubble Sizes. . . . .	78
F. Effect of Surface Aeration. . . . .	79
G. Exponents of $N^3 D^2$ , and $N_{Re}$ . . . . .	80
H. Exponents of $V_S$ . . . . .	82
I. Exponents of $T$ . . . . .	83
J. $N^3 D^2$ for the Gas Agitation Region . . . . .	84
K. Values of the Correlation Constant. . . . .	86
L. Comparison of the Experimental and Calculated $k_L a$ 's . . . . .	89
NOMENCLATURE . . . . .	92

LIST OF TABLES

Table	Page
I. Gas Hold-up, Experimental Correlations. . . . .	23
II. Specific Interfacial Area, Experimental Correlations. . . . .	24
III. Volumetric Mass Transfer Coefficient, Experimental Correlations. . . . .	25



## LIST OF FIGURES

Figure	Page
1. Experimental Apparatus. . . . .	30
2. Effect of Mechanical Agitation on $k_L a$ ; $T = 10^\circ\text{C}$ . . . . .	44
3. Effect of Reynolds Number on $k_L a$ ; $T = 10^\circ\text{C}$ . . . . .	45
4. Effect of Agitator Speed on $k_L a$ ; $T = 10^\circ\text{C}$ . . . . .	45
5. Effect of Agitator Speed on $k_L a$ ; $T = 10^\circ\text{C}$ . . . . .	48
6. Effect of Solid Particles on $k_L a$ 's of Small Bubbles; $T = 10^\circ\text{C}$	50
7. Effect of Solid Particles on $k_L a$ 's of Large Bubbles; $T = 10^\circ\text{C}$	51
8. Effect of Superficial Gas Velocity on $k_L a$ ; $T = 10^\circ\text{C}$ . . . . .	53
9. Effect of Temperature on $k_L a$ ; $V_s = 2.73$ cm./min. (LBNP) . . . . .	53
10. Effect of Temperature on $k_L a$ ; $V_s = 2.73$ cm./min. (SBNP) . . . . .	53
11. Comparison Between the Dependencies of the Air Agitation and Transition Points on $V_s$ ; $T = 10^\circ\text{C}$ . . . . .	57
12. Dependency of $k_L a$ on $V_s$ With No Mechanical Agitation. . . . .	59
13. Dissolved Oxygen Analyzer Calibration Chart . . . . .	70
14. Raw Data Plot for $k_L a$ Determination . . . . .	71

## CHAPTER I

### INTRODUCTION

Many chemical processes include a reaction between a gas and a liquid, or something which is suspended in the liquid, e.g., a colloid. One of the most important problems in such a reaction is the choice of the method used in putting the gas in contact with the liquid. This problem is much more serious when the rate of mass transfer from the gas phase into the liquid phase is very low, and the rate of the process is determined by this transfer rate. One way to increase the rate of transfer of the gas into the liquid in such processes is to bubble the gas through the liquid in an agitated vessel designed for this purpose. One system that has been of rather high interest to the researchers in the past two decades has been the agitated gas-liquid contactors used in the aeration of water.

Aeration of water is an important topic in the fields of industrial fermentation and industrial wastes, and sewage treatment. It has been remarked that,

In present day bubble aeration practice only a small percentage of the oxygen supplied to the system is absorbed by the tank liquid from the dispersed bubbles; any means whereby this percentage is increased....will result in substantial reduction in operating costs, other conditions being equal (12).

The investigations that have been performed on this subject have mostly been directed towards a better understanding of the oxygen transfer from the gas bubbles, the bubble characteristics, and the

determination of characteristic variables of the mechanically agitated gas-liquid contactors. From these previous investigations it can readily be seen that the process of bubble aeration is rather complicated. Furthermore, due to this complicated nature of the process, the interpretations of the experimental results differ among various researchers, even though the results themselves sometimes agree closely.

Bubble aeration of water was chosen for study in this investigation for the following reasons:

1. To determine whether solid particles in the agitated media, i.e. water, would increase the over-all mass transfer rate. It was thought that this increase might occur as a result of either one or both of the following two phenomena: (a) increase in the bubble breakage due to an increase in the agitation because of the particles, and (b) increase in the bubble breakage due to the direct collisions of the rising bubbles with the moving particles. In short, it was hoped that the solid particles would act as moving baffles;
2. To check the results of the previous investigations against the range of variables in this investigation;
3. To propose explanations for the experimental results obtained in this work, and also to derive a correlation giving the transfer coefficient and interfacial area product as a function of the system variables.

This work is different from many others in that only air and water were used, and the dissolved oxygen was measured by an oxygen analyzer. Others usually used a sulfite solution, rather than water, in an effort

to determine the amount of oxygen that was transferred into the liquid during the aeration period. This work, therefore, eliminated the uncertainty of extending the results of the oxygen transfer into sulfite solution to oxygen transfer into water.

## CHAPTER II

### A SURVEY OF THE LITERATURE

Investigations on mass transfer from the gas phase into the liquid phase have been conducted for different systems under different conditions, but all for the purpose of understanding the mechanism of this transfer. These studies can be divided into two areas: Those gas-liquid mass transfer processes accompanied by a chemical reaction and as those in which no reaction takes place. Furthermore, different types of gas-liquid contacting systems, such as tray columns, wetted-wall towers, packed columns, spray columns, surface contactors, and agitated vessels have been used in these studies. Another difference among these studies is that some were made with mechanically undisturbed systems while others have been conducted with mechanically agitated systems. Another point of diversification among these investigations is that some studied the over-all behavior of the contacting system, while others studied the behavior of the individual phases.

The system under consideration in this work concerns the transfer of a sparingly soluble gas from a gas bubble into the liquid media, namely, the transfer of oxygen to water from the bubbles of air bubbling through water. The published theoretical considerations of this process dates as far back as 1878 and is due to Stefan (64) although it is evident that even before Stefan's time this process was known. What Stefan seems to have done is to have deduced from Fick's law

relationships for this type of mass transfer.

The actual mechanism of transfer was explained at different times by different models (13, 31, 40, 41, 48, 73). However different they may be, all of the explanations for this transfer seem to agree on the equation:

$$\frac{dC_L}{dt} = kA(C_S - C_L) \quad \text{II-1}$$

where  $C_S - C_L$  is the driving force causing the transfer of matter,  $k$  is the transfer coefficient,  $A$  is the transfer area,  $t$  is the time, and  $C_S$  and  $C_L$  refer to the oxygen concentration in the liquid phase at saturation and at any time, respectively. Below is a short summary of the existing theories on  $k$  that have been derived from different proposed mechanisms of transfer.

#### Two Film Theory

The two film theory was proposed by Lewis and Whitman (40, 73). It assumes that adjacent to both sides of the gas-liquid interface around the gas bubble there exists two layers, one of gas and the other of liquid, in which mixing can be assumed to be non-existent. Perfect mixing is assumed in both the bulk of the gas bubble and also in the bulk of the liquid. They also assumed that resistance to the diffusion of the gas molecules from the gas phase into the liquid phase lay totally in these two stationary layers. Furthermore, they postulated that the liquid-film resistance was much greater than the gas film resistance, since the number of collisions are much larger in the liquid film. The main assumption in this theory is that the transfer coefficients are assumed to be inversely proportional to the film thickness and directly

proportional to the diffusivity of the gas in the liquid:

$$k = \frac{D}{\delta} \quad \text{II-2}$$

With the assumption that the liquid film resistance is the predominating factor opposing the transfer, the transfer equation can be written as follows:

$$\frac{1}{a} \frac{dC_L}{dt} = k_L (C_G - C_L) \quad \text{where} \quad k_L = \frac{D}{\delta_L} \quad \text{II-3}$$

Inherent in the above equation is the assumption that the liquid surface on the interface is substantially saturated with the gas, due to the considerably higher resistance on the liquid side. Therefore, for gases of low solubility, such as oxygen in water, the rate of transfer is very slow. As a result, only a small concentration difference develops across the interface.

According to the 'two film theory' the stationary film resistance could be decreased by cutting down the film thickness. Assuming  $D$  is constant, this would increase the value of the transfer coefficient  $k_L$  (liquid side).

#### Penetration (Surface Renewal) Theory

The 'two film theory' was introduced in 1923-1924. In 1935 Higbie (31) proposed that the two film theory "... is not valid for the prediction of the effect of diffusivity ..." for the 'penetration period.' He derived an equation for 'short contact times' from Fick's second law:

$$k_L = 2\sqrt{\frac{D}{\pi t_e}} \quad \text{II-4}$$

Thus, the transfer equation could be written as

$$\frac{1}{a} \frac{dC_L}{dt} = 2\sqrt{\frac{D}{\pi t_e}} (C_s - C_L), \quad \text{II-5}$$

where  $t_e$  is the 'exposure time.' This theory makes the assumption that fresh layers of liquid are brought into contact with the gas for a limited period of time. Higbie assumed this time of contact, i.e., exposure time, is equal for each layer. The fluid layer is considered to be quiescent during this time of contact, and the gas is transferred by molecular diffusion in a direction perpendicular to the interface. The theory was developed for the contact of pure gas bubbles with a liquid, thereby eliminating the gas film resistance. For exposure times longer than the penetration period, Higbie's 'penetration mechanism' gives identical results to those obtained from the two film theory; i.e., the 'penetration' results approach the 'film' results as the exposure time comes closer to the 'penetration period.'

The 'penetration theory' was modified in 1951 by Danckwerts (13), who relaxed the restraining condition that the exposure time for all layers is constant. This modified mechanism is more commonly known as the 'surface renewal model' and considers a distribution of the contacting times. Therefore, if there are bubbles of different exposure times ('age groups'), then it can be said that the supply of fresh liquid surface to each bubble, i.e., "the rate of production of fresh surface," is not the same for all bubbles. Such a consideration gives

$$\frac{dC_L}{dt} = \sqrt{\frac{D}{\pi t_e}} (C_s - C_o) F e^{-Ft_e} dt_e \quad \text{II-6}$$

When the above equation is integrated with respect to  $t_e$  over the whole range of the  $t_e$  distribution, i.e.,  $0 \leq t_e \leq \infty$ , the mean rate of absorption is found to be

$$\frac{dC_L}{dt} = (C_s - C_o) \sqrt{DF} \quad \text{II-7}$$

where  $F$  is the mean rate of production of fresh surface. Thus,  $\sqrt{DF}$



can be identified with  $k_L$ .

### Boundary Layer Theory

In the derivation of his 'penetration theory' for gas liquid mass transfer Higbie (31) included the assumption that during the time of contact while the transfer of matter is taking place between two phases, the liquid layer in contact with the gas would be stationary. This assumption is justified in the case of some gas-liquid transfer operations, but not in others. The 'boundary layer theory' relaxes this restraint and assumes that a fluid velocity component exists along the interface in a direction perpendicular to the direction of mass transfer. It further assumes that during the exposure time the diffusing gas penetrates into the liquid boundary around the gas bubble to a distance equal to or smaller than the distance between the interface and a point in the boundary layer where  $u/u_\infty = 0.5$ , where  $u$  is the velocity of the liquid transverse to the direction of mass transfer at a point in the boundary layer, and  $u_\infty$  is the fluid velocity in the same direction as  $u$  at a distance equal to or greater than the laminar boundary layer thickness. It can be shown that if the above assumptions are incorporated with the laminar boundary layer equations, one obtains an equation for the  $k_L$  which shows that  $k_L$  is proportional to the two-thirds power of the diffusivity of the gas in the liquid (46),

$$k_L \propto D^{2/3}. \quad \text{II-8}$$

Besides the above mentioned modifications of the 'penetration theory' there are other modifications, one of which is due to Levich (41). In 1953 Pasveer (52, 53) proposed a theory which considers the diffusion of the gas through the monomolecular layers of fluid which

gives the same final result as the 'penetration' theory. This line of thought, although giving the same final answer, was claimed to be independent of that of Higbie's (31).

#### Kinetic Theory of Gas Absorption

The 'kinetic' theory was developed by Miyamoto (48) in 1932. It is based on the idea that only a fraction of the gas molecules in the gas phase and a fraction of those gas molecules dissolved in the liquid phase have a velocity component perpendicular to the point of contact on the interface above a 'threshold' velocity  $u_0$  for the molecules on the gas side, and  $u_0'$  for the molecules on the liquid side. According to this theory, only those molecules of gas with velocities above their respective 'threshold' velocities can pass across the interface, and the net amount absorbed from the gas bubble is the difference between these two quantities of transferred molecules. This theory is neither as well known nor as popular as the previously mentioned ones. Its derivation includes the kinetic theory of gases and makes use of the Maxwell velocity distribution.

From the above discussion on the theories of gas-liquid mass transfer it can easily be seen that there are several ways with which the results of experiments can be explained. Each case, however, depends to some extent upon the operating conditions and the equipment.

#### Bubble Characteristics

From the many investigations on bubble characteristics, it can be seen that although numerous correlations and theoretical equations have been proposed, a general description of bubble characteristics has not

yet been found. Investigators have claimed that the physical properties of both the continuous and the discontinuous phases, sparger characteristics, container characteristics, and operating conditions such as the temperature, agitation rate, gas flow rate, etc., all affect the bubble behavior in one way or another.

Haberman and Morton (28) have reported that it is not possible to describe the motion of the air bubbles completely by the use of the dimensionless parameters which include the usual physical properties of the liquid.

The size of the gas bubbles formed under a liquid is determined by the balance between the bouyant force separating the bubble from the orifice, and the shearing force necessary to break the surface tension across the orifice. Quigley, Johnson, and Harris (58) have found that the viscosity and the density are not important factors in the determination of the bubble size, but that the orifice diameter and the gas flow rate are the controlling factors. Leibson, Holcomb, Cacosso, and Jacmic (39) have reported the following equation for the air bubbles formed under high liquid seals, and in laminar flow:

$$D_B = 0.18 D_o^{1/2} N_{Re}^{1/3} \quad \text{II-9}$$

where  $D_B$  is the bubble diameter,  $D_o$  is the orifice diameter, and  $N_{Re}$  is the Reynolds number; i.e., bubble diameter is a function of the mass rate of gas flow, orifice diameter, and viscosity. They have also noticed that in the laminar region and at a given Reynolds number the bubble sizes were uniform. Van Krevelen and Hoftijzer (67) have reported that two types of gas bubbles in liquids can be distinguished: those bubbles which are formed separately, and those bubbles which are formed in series (chain bubbling). They have also found that for a given

orifice the 'chain bubbling' starts after a critical gas flow rate, and that for such bubbles the bubble diameter is independent of the orifice diameter and is a function of the gas flow rate (bubble size increasing with the gas flow rate). For the separately formed bubbles they have found that the bubble size is almost independent of the gas flow rate and is a function of the orifice diameter. West, Gilbert, and Shimizu (69) also reported similar results.

The shape of the bubbles, furthermore, is a function of their size in a given gas and a liquid. It has been found that small bubbles have spherical shapes, larger ones are ellipsoidal, and even larger ones are spherical caps (28, 39, 41).

The velocity of rise of the gas bubbles in the liquid is a function of the bubble size, gas velocity, and the liquid characteristics. The rising velocity of the bubbles formed at higher gas rates are higher than those formed at the lower gas rates due to the proximity of the bubble formation, and also due to the disturbances caused by the bubble wakes (19). The velocities and shape characteristics of air bubbles in water can be related to a modified Reynolds number as shown by Haberman and Morton (28). Van Krevelen and Hofjitzer (67) have shown that for 'chain bubbling' the velocity of rise is a function of the gas flow rate and the gas hold-up in the liquid, and from this that the velocity is a function of the bubble diameter and the gas flow rate. Furthermore, it should be noted here that a gas bubble during its period of rise does not have the same velocity at all times. It starts rising with a velocity which is different from the velocity it attains later during the rise; i.e., its initial velocity differs from its terminal velocity.

When a gas bubble is formed and starts rising through the liquid

above it, the bulk of the gas in the bubble and the liquid surrounding it are not in a state of rest. The gas inside the bubble has circulatory currents (14, 41), and the liquid surrounding it is in turbulent motion. The circulation in the bubble is not directly related to the present work and will not be discussed here. The turbulence in the liquid medium, due to the motion of the bubbles, is a function of the physical properties of the gas and the liquid, the gas velocity, the sparger, and the bubble size. Hixson and Gaden (33) used two different kinds of spargers, single bubble and fine bubble, and noticed that at low air rates the bubbles formed from both of the spargers caused limited turbulence, but at high air rates the single bubble sparger caused much greater turbulence in the liquid than the fine bubble sparger. Calderbank and Moo-Young (9) used sieve plates and found that the power input per unit volume of liquid (another way of expressing the turbulence) for air agitation only is a function of the superficial gas velocity for a given liquid. It should be evident from the above discussion that the terms 'turbulence' and/or 'agitation' mean the disturbances caused by the bubbles only, since no mechanical agitation effects are considered in the above discussion. Other work along similar lines are reported in the literature (14, 28, 37).

#### Stages of Bubble Life

The life of the bubble from the time it starts to form at the sparger submerged in the liquid until it breaks up at the gas-liquid interface at the top, undergoes three distinct stages. These stages are: (a) the formation stage, (b) the stage of free rise, and (c) the coalescence stage. The bubble has different characteristics in each of

these three stages and thus the gas liquid mass transfer is not the same in all three stages. Early studies on the different stages of the bubble life were conducted by Whitman, Long and Wang (74); they studied the mass transfer from spray droplets. Some of the later studies were done by Licht and Conway (42), Licht and Pansing (43), Dixson and Russel (17), Dixson and Swallow (18), Popovich, Jervis and Trass (56), and others (10, 14). These investigators have found that about 10-50% of the mass transfer occurs during the formation stage, the percentage varying with the systems and operating conditions. The high rate of gas absorption during the formation period as the bubble emerges from the orifice has been attributed to the rapid and continuous replenishment of the air-water interface (19, 56). During the free-rise period following the bubble formation, the mass transfer rate across the gas-liquid interface seems to be smaller and relatively constant (19). During the coalescence period the transfer rate is higher than it is in the free-rise period (19). Also, some surface aeration may take place at the very end of the bubble life due to the bursting of the bubble at the surface (10, 14, 19, 56).

#### Nature of the Transfer Coefficient

As was mentioned before, there are three different resistances in series for the case of the absorption of oxygen from air by water. In the present case the gas side resistance may be neglected (7, 10, 33, 38, 75, 76). This condition is true in the case of the diffusion of a gas from a bubble which contains only one component, and it is a good approximation for the absorption of a sparingly soluble gas by a liquid from a gas mixture, i.e., oxygen into water from air (7, 21, 34,

75, 76). Similarly, the interfacial resistance is also neglected and in most cases it is not even mentioned; Chiang and Toor (11) have shown that although interfacial resistance is present, it can be neglected. Now, after eliminating two of the three resistances we see that the transfer coefficient can be correlated as a function of the liquid side resistance only; i.e., we only need to consider the liquid side mass transfer coefficient,  $k_L$ .

The effect of the solubility of the gas on the transfer coefficient is very slight. Hammerton and Garner (29) found that  $k_L$  is only slightly affected by the solubility of the gas, and they also found that  $k_L$  is independent of the concentration of the inert gases in the bubble or in the liquid over a range of partial pressures from 10 to 500 mm. of mercury. This behavior may be predicted from the theory. If one takes Higbie's definition for the transfer coefficient, equation (II-4), as the reference for discussion, one can easily see that the solubility of the gas in the liquid has very little effect on the transfer coefficient, since no term for the driving force appears in the equation. Other equations for the transfer coefficient show similar behavior. This phenomenon can be explained by the fact that the effect of the concentration of the dissolved gas on the diffusivity is very slight under normal conditions (15), because the viscosity of the solution, as well as its density, is essentially the same as the pure solvent under these conditions (15). This is a particularly valid assumption in the case of a sparingly soluble gas such as oxygen in water.

The effect of temperature on the transfer coefficient was found to be much less than that predicted by the temperature dependence of diffusivity alone. If one considers Higbie's definition for  $k_L$  and

assumes that  $t_e$  is constant with temperature, one will find that the increase in the diffusivity of oxygen in water with temperature is not reflected in  $k_L$  as much as would be expected. This leads one to the conclusion that the exposure time is indeed a function of the temperature due to its dependence on the liquid properties. Experiments were performed for the purpose of studying the effect of temperature on  $k_L$  and  $k_L a$  (29, 75, 76). One of these investigations (28) has shown that for bubbles with diameters 0.6 cm. or larger, the effect of temperature on the  $k_L$  is very slight at room temperatures. It was also found that for smaller bubbles and lower temperatures ( $<17^\circ\text{C}$ ), the temperature effect was larger.

Another system variable is mechanical agitation, which is commonly used in the gas-liquid contactors. This agitation serves to produce additional turbulence in the liquid. If one considers the surface renewal model (13), where  $k_L$  is equal to the square root of the product of the diffusivity and the mean rate of surface renewal, it may seem that the effect of the surface renewal rate and the effect of the diffusivity will hold as stated for all degrees of turbulence. This assumption seems to be wrong since the effect of the diffusivity is decreased as the turbulence increases, and the transfer coefficient is more and more dependent on the surface renewal rate. What is happening in this case is that the exponent of the diffusivity is being decreased from 0.5 as it is stated in Danckwerts' equation to about zero at very high turbulence. Furthermore, in the cases where turbulence is very low, it was shown that (65) the Lewis-Whitman theory (two film theory) holds. From the above brief discussion it can be gathered that  $k_L$  is affected by turbulence (although not very much), which in fact changes the



mechanism of transfer, i.e., changes the weight of the different variables for different agitation rates. Calderbank and Moo-Young (9), Johnson, Saito, Polese and Hougen (36) and Yoshida, Ikeda, Imakawa, and Miura (76) have studied the effect of turbulence on the  $k_L$ . These investigations showed that the transfer coefficient is increased by increased turbulence in the liquid, but this dependence on turbulence is not always appreciably large.

The effect of the bubble size on the transfer coefficient is also a point of dispute among several investigators. Some (10, 19) claim that  $k_L$  is a function of the bubble size, whereas rather recent papers by Calderbank and Moo-Young (9) and Hyman (35) report that the transfer coefficient is not a function of the bubble size. In the same paper, however, they seem to contradict their conclusion about the 'independence' by giving two different correlations for  $k_L$ : one for small bubbles and another for large bubbles (9).

Studies on Oxygen Absorption by Water from  
Bubbles in Agitated Gas-Liquid Contactors

Oxygen absorption in agitated gas-liquid contactors has been studied by a number of investigators. A summary of the results of these previous studies is given in Tables 1, 2, and 3. The results of the present work are included in Table 3. Most of these investigations were performed to get correlations for the transfer coefficient as a function of variables such as the superficial gas velocity, power input or stirrer speed, geometry of the vessels, liquid height and other operating and system variables. Most of these works have used one or more types of impellers, and most of these investigations have been performed along the lines of

the pioneering work of Cooper, Fernstrom, and Miller (12) for evaluation of the vessel, operating conditions, and impellers. Furthermore, Cooper, et al. have used the technique known as the 'sulfite oxidation method,' as developed by Miyamoto (47, 48, 49). Miyamoto's investigation was not done with the purpose of obtaining a correlation for an agitated vessel, but with the purpose of studying the diffusion rate of oxygen into sodium sulfite solution. Miyamoto reported that the dissolution velocity was a linear function of the partial pressure of the oxygen in the gas bubble. As was mentioned above, Cooper, et al., (14) were the first to publish a correlation for gas-liquid contactors for air bubbling through a sodium sulfite solution. They correlated their transfer coefficient data with the power input to the agitator and also with the superficial gas velocity for a vaned disc:

$$k_L a = C P_v^{0.95}, \text{ and} \quad \text{II-10}$$

$$k_L a = C' V_s^{0.67} \quad \text{II-11}$$

As can be seen from the above equations, the correlation is not really for the transfer coefficient but rather for the product of the transfer coefficient and the interfacial area. This product,  $k_L a$ , is generally used in these correlations due to the difficulty in determining the correct interfacial area. Cooper, et al., (12) noted that the latter of the above two equations was valid up to a 'loading point'; after which the experimental values of  $k_L a$  were lower than those predicted by the correlation. This 'loading point' was defined as the air rate above which the gas was no longer uniformly dispersed by the agitator. Above

---

\* Cooper, et al., (12) reported their correlations for a volumetric transfer coefficient,  $k_v$ , which can be reduced to  $k_L a$  by means of a constant multiplier.

this air rate much of the gas escaped around the edge of the impeller and rose in large bubbles or clusters around the shaft.

Friedman and Lightfoot (25) also studied oxygen absorption in agitated tanks and found that over most of the range of their experiments  $k_L a$  was independent of  $V_s$  except at low impeller speeds. They also found that the power input per unit volume varied as the 2.1 power of the speed (revolutions per minute) of the agitator at low air rates, and as the 2.4 power of the speed at high air rates. Another thing that they noticed from their studies was that for a given stirrer speed the power input to the impeller decreased with increased air flow rate. After a certain point an increased gas flow rate had no effect on the power input. This phenomenon was explained by the observation that the fractional air hold-up remained constant above a certain air flow rate. This behavior is reflected in the following equation which gives the power input to a liquid in turbulent flow (with mechanical agitation):

$$P = \frac{C}{g_c} N^3 D^5 \rho \quad \text{II-12}$$

In the above equation the density term becomes constant above the point where the hold-up ceases to increase with increasing gas flow rate. Furthermore  $\rho$  is a function of the Reynolds number ( $N_{Re} = \frac{dN}{\mu}$ ), and above this critical point it, too, becomes constant because the physical properties  $\rho$  and  $\mu$  do not change. From their study Friedman and Lightfoot (25) concluded that the best correlation for a paddle impeller was

$$k_L a = CN^3 D^5 \quad \text{II-13}$$

Hixson and Gaden (33) studied the absorption of oxygen from air bubbles in cultures of baker's yeast. They used two types of spargers, as mentioned before. For the single bubble sparger with mechanical

agitation, they found

$$k_L a = CV_s^{0.68} \quad \text{II-14}$$

This result is almost exactly the same as that found by Cooper, et al., (12) for non-biological systems. For air agitation only they reported two more correlations, one for each type of sparger used:

$$k_L a = CV_s^{0.82} \quad \text{II-15}$$

$$k_L a = CV_s^{0.33} \quad \text{II-16}$$

which hold for single bubble and fine bubble spargers respectively.

Maxon and Johnson (44) and Bartholomew, Karow and Spat (1) also studied the characteristics of gas-liquid contactors for biological cases. Maxon and Johnson (44) found that

$$k_L a = CV_s^{0.40} \quad \text{and} \quad \text{II-17}$$

$$k_L a = CN^{1.70} \quad \text{II-18}$$

They concluded that the sulfite oxidation method used by many other investigators is not adequate for the evaluation of fermentors. This conclusion was also reported by Schultz and Gaden (60). Bartholomew, et al., (1) used an amperometric technique for the oxygen determination in their fermentor and found that for a given stirrer speed and air flow rate the transfer coefficient and interfacial area product was much greater for smaller bubbles than for larger bubbles. They concluded that this behavior was due to the fact that larger bubbles rise faster and also have a smaller interfacial area per unit volume. Thus the larger bubbles do not contribute as much exposure time or area for mass transfer. They also stated that mechanical agitation may influence the hold-up and the residence time of the bubbles. They found that for a given stirrer speed and increasing air flow rate, the transfer coefficient at first increased rather steeply then became asymptotic to a

final value.

Elsworth, Williams and Harris-Smith (21) experimented with different impeller speeds, air rates, and impeller diameters, and reported that they obtained straight lines with positive slopes when they plotted the stirrer speed versus the absorption coefficient. They obtained a correlation which showed  $k_L a$  proportional to the stirrer speed taken to the 2.4 power.

Hyman and Van Den Bogaerde (34) studied the absorption of oxygen by sulfite solutions and found that  $k_L a$  is dependent on the stirrer speed, stirrer diameter, superficial velocity, liquid height, and tank diameter in the following manner:

$$k_L a = C(ND)^{2.18} v_s^{0.17} \left(\frac{Z}{T}\right)^{-0.50} \quad \text{II-19}$$

They also stated that  $k_L a$  is not significantly affected by temperature at the two different temperatures they ran, 20 and 35°C. Another point that they reported seems to be rather interesting: in their case the  $k_L a$  values did not show any change for two different types of spargers, a fritted glass sparger and an open tube sparger.

Yoshida, et al., (76) also investigated oxygen transfer from air bubbles into a sulfite solution. Their data was correlated as

$$k_L a = C v_s^m (N^3 D^2)^n \quad \text{II-20}$$

where the exponents  $m$  and  $n$  were found to be different for different operating conditions for the vaned disc. For the turbine  $n$  and  $m$  were equal to 2/3. They were satisfied with this correlation since "the data for the three vessels of different sizes fall on the same line for a given gas velocity" (76). They also noticed that the  $k_L a$  values for the 4 mm. nozzle were slightly higher than those for the 8 mm. nozzle, but this difference was negligible at high agitator speeds. They furthermore

noted that  $k_L a$  decreases with increasing viscosity, but the exact effect of viscosity on  $k_L$  could not be determined since the bubble area might also be affected by viscosity. In the range of their experiments they found that the  $k_L a$  values at 20 and 40°C were the same, but that there was a 25% increase in the  $k_L a$  values between the runs at 7 and 20°C. In a recent work Yoshida, et al., (75) have reported that for an air-sodium sulfite solution system higher  $k_L a$ 's were obtained for higher temperatures. They ran at 10, 20 and 30°C.

A study by Westerterp, Van Dierendonck and Dekraa (72) proposed that the gas-liquid contactors may be considered in two regions, according to the stirrer speed. The first region is the one in which the stirrer does not appreciably contribute to the agitation. In this region the agitation and the interfacial area is predominantly governed by the gas load. For stirrer speeds higher than a critical speed, ( $n_0$ ), agitation and interfacial area are a function of the mechanical agitation and are independent of the gas rate.

Becker (2) also worked on oxygen absorption in agitated vessels and found that when the rate of solution was plotted against the rate of stirring a straight line was obtained. However, when the effect of the variations in interfacial area produced by stirring was taken into account, a curve resulted. This curve showed that with increased stirring the transfer rate does not increase indefinitely but tends to reach a plateau.

Karwat (37) also studied a similar problem. His investigations showed that the  $k_L a$  values for the small bubbles were larger than the  $k_L a$  values for the large bubbles at low agitation rates. Also, he showed that as the agitation rate was increased, the  $k_L a$  for the

bubbles produced from a single-opening sparger approached the values obtained from a fritted disc sparger. For air agitation only his data showed a relationship for turbulence due to gas flow similar to that observed by Calderbank (9).

Interfacial area in the agitated gas-liquid contactors has been studied by Calderbank (6, 7, 8, 9), Yoshida and Miura (77), Vermeulen, Williams and Langlois (68) and others (8, 9, 57). Results of these experiments have shown that the interfacial area is a function of the sparger, gas flow rate, and agitation rate, but that the contribution of each variable tends to change with varying operating conditions.

In recent years some workers (27, 30) have studied the effect of agitation on residence time in an effort to correlate the transfer rate with residence time, and developed a model for the agitated gas-liquid contactors based on the residence time (26).

Before concluding this section it would be proper to draw the attention of the reader to the following points:

1. Although a great deal of work has been done in the last two decades, neither a clear understanding of the mechanism of the gas-liquid mass transfer nor a general design equation for gas-liquid contactors have been developed. There is still a high degree of confusion in the available literature.
2. No investigation of gas-liquid mass transfer in the presence of solid particles was noticed.

TABLE I. GAS HOLD-UP, EXPERIMENTAL CORRELATIONS

Variable Correlated	Range of Experiments				Type of Correlation, Exponent of			Vessel Volume $\times 10^3$ (ft <sup>3</sup> )	D' / T	Tank Diameter T (ft)	Impeller		Sparger		System		Reference
	V <sub>g</sub> (ft/min)	RPM	P/V (HP/ft <sup>3</sup> )	$\beta$ (%)	V <sub>g</sub>	RPM	P/V				Type	Number of Blades <sup>a</sup>	Diam.	Number of Holes	Liquid	Gas	
$\beta$	0 - 2.4	0	0	0 - 28	1.0	-	-	?	0	0.148; 0.165	None	None	Fritted Glass	Water	Air	(22)	
$\beta$	0 - 12	0	0	0 - 17	1.0	-	-	1749; 9680	0	1.49; 3.53	None	None	0.02"; 0.03"	47	Water	Air	(22)
$\beta$	0 - 12.5	0	0	0 - 38	1.0	-	-	{ 4.24; 8.48 }	0	1.65	None	None	Perous Plates	Water	{ CO <sub>2</sub> ; H <sub>2</sub> }	(61)	
$\beta$	12.5 - 30	0	0	38 - 32	0 - (-1)	-	-	{ 4.24; 8.48 }	0	0.53	None	None	Perous Plates	Water	{ C <sub>2</sub> H <sub>2</sub> ; SO <sub>2</sub> }	(61)	
$\beta$	0.6 - 3.6	0	0	0 - 7	1.0	-	-	22.2; 367.2	0	0.66; 1.68	None	None	1/8"	100	Ethyl Acetate; m-xc Ethanol; Glycol	Air	(6)
$\beta$	12 - 120	0	0	8 - 60	?	-	-	2.47; 14.84 (7)	0	1.214; 0.462	None	None	1/8"	1 - 3/4 holes/in <sup>2</sup>	Glycol; Glycerol	CO <sub>2</sub>	(7)
$\beta$	0.4 - 36	0	0	0.8 - 20	0.84	-	-	1.06 - 4.24	-	0.208	None	None	1 - 9.6 mm	1	Water	Air	(58)
$\beta$	0.5 - 4.5	0	0	1.5 - 10	0.8	-	-	0.88 - 1.09	0	0.68; 0.155; 0.254	None	None	0.55 - 6 mm	1	Water	Air	(67)
$\beta$	0.11 - 5.5	0	0	1.5 - 8	0.9	-	-	{ 15.5 - 318 }	0	0.254	None	None	{ 2.25 - 40mm }	1	{ Water; } { Sulfite }	{ Air } { O <sub>2</sub> }	(75) (75)
$\beta$	11 - 55	0	0	12 - 40	0.43	-	-	{ 15.5 - 318 }	0	1.98	None	None	{ 2.25 - 40mm }	1	Sulfite	Air	(27)
$\beta$	0.76 - 3.2	78 - 340	0.007 - 0.036	0.9 - 11	0.55	-	-	170.2	0.4	1.29	Vaned Disc	16	3/8"	1	Sulfite	Air	(77)
$\beta$	0.33 - 1.5	60 - 350	-	0.3 - 5	0.49 - 0.61	0.8 - 0.6	-	{ 42.4; 159; 555 }	{ 0.4 } { 0.4 }	0.826; 1.239 1.93	Vaned Disc	16	4, 8, 12 mm	1	{ N <sub>2</sub> OH } { H <sub>2</sub> O } { Glycerol }	{ CO <sub>2</sub> }	(77)
$\beta$	0.33 - 1.5	60 - 350	-	0.4 - 5	0.75	0.6	-	{ 42.4; 159; 555 }	{ 0.4 }	1.239	Turbine	12	4 mm	1	Glycerol	?	(53)
$\beta$	?	?	?	?	0.7 - 1.0	0.5	?	6.71	0.7	0.429	Turbine	2	?	?	?	?	(8)
$\beta$	0.6 - 3.6	-	0.01 - 0.2	0 - 8	0.5	-	-	22.2; 367.2	0.33	0.66; 1.68	Turbine	6	1/8"	1; ?	Ethyl Acetate EtOH, H <sub>2</sub> O; Glycol	Air	(8)
$\beta$	1 - 5.0	85 - 854	0.007 - 0.02	2 - 10	0.53	-	-	77.6; 29700	0.33; 0.2	0.99; 805	Turbine	6, 10	?	4	Water	Air	(23)
$\beta$	0 - 3.3	135- 790	-	-	0.6	0.5	-	6.71	0.7	0.429	Turbine	?	0.0135"	25	$\alpha$ - Methyl Styrene	H <sub>2</sub>	(36)
$\beta$	2.34	300 - 2200	-	3 - 32	?	1.0	-	10.1	0.4	0.628	Turbine	6	?	?	Sulfite	Air	(70)



TABLE II. SPECIFIC INTERFACIAL AREA, EXPERIMENTAL CORRELATIONS

Variable Correlated	Range of Experiments				Type of Correlation; Exponent of				Vessel Volume $\times 10^3$ ft <sup>3</sup>	$\frac{D}{T}$	$T$ (ft)	Impeller		Sparger		System		Reference
	$V_s$ (ft/min)	RPM	P/V (HP/ft <sup>3</sup> )	$\beta$ (%)	$\beta$	$V_s$	RPM	P/V				Type	Number of Blades	Disn.	Number of Holes	Liquid	Gas	
a	0 - 3	0	0	0 - 7	0.5	0.704	-	-	6.7	0	0.5 x 1.68	None	None	1/8"	100	Water	Air	(6)
a	12 - 120	0	0	8 - 60	-	0.9	-	-	2.47; 14.8 (?)	0	0.214; 0.462	None	None	1/8"	1 - 3W/in <sup>2</sup>	Glycerol Glycerol, H <sub>2</sub> O	CO <sub>2</sub>	(7)
a	18 - 102	0	0	50 - 80	-	0.9	-	(0.4)	9.5	0	0.33 x 0.29	None	None	1/16"; 1/32" 1/8"	18 - 98	Glycerol Glycerol, H <sub>2</sub> O	Air; CO <sub>2</sub>	(9)
a	0.1 - 4.5	0	0	0.8 - 8	-	0.715	-	-	1.06 - 4.4	0	0.228	None	None	1 - 9.6 mm	1	Water	Air	(38)
a	0.5 - 4.5	0	0	1.5 - 10	-	0.40	-	-	0.92 - 11	0	0.086; 0.155; 0.254	None	None	0.55 - 6 mm	1	Water	Air	(67)
a	0.33 - 1.5	60 - 350	-	0.3 - 11	-	0.33 - 0.66	0.9 - 0.7	-	42.4 - 159	0.4	0.826; 1.237	Vaned Disc	16	4, 6, 12 mm	1	NaOH, H <sub>2</sub> O	CO <sub>2</sub>	(77)
a	0.33 - 1.5	60 - 350	-	0.3 - 14	-	0.74	1.1	-	574.5	0.4	1.930	Turbine	12	4 mm	1	Glycerol	CO <sub>2</sub>	(77)
a	0.6 - 7.6	-	0.01 - 0.2	0 - 8	0.5 (?)	0.50	-	0.40	22.3; 367	0.33	0.094; 1.682	Turbine	6	1/8"	1; (?)	H <sub>2</sub> O, EtOH Glycerol	Air	(6)
a	0.6 - 3.6	-	0.01 - 0.2	0 - 8	0.35	0.50	-	0.40	22.3; 367	0.33	0.694; 1.682	Turbine	6	1/8"	1; (?)	Alcohols	Air	(6)
a	0.6 - 3.6	-	0.01 - 0.2	0 - 8	0.65	0.50	-	0.40	22.3; 367	0.33	0.694; 1.682	Turbine	6	1/8"	1; (?)	Electrolytes	Air	(6)
a	0.6 - 3.6	-	0.01 - 0.2	0 - 8	-	-	-	-	17.7 - 367	0.33	0.5 - 1.682	Turbine	6	1/8"	1; (?)	Glycerol, H <sub>2</sub> O	CO <sub>2</sub>	(7)
a	?	?	?	?	?	0.60	?	0.35	155.3	0.33; 0.40 0.47	1.255	Paddle	5	?	?	?	?	(57)
a	-	100 - 400	-	2 - 30	$\beta$ 2.58 + 0.75	-	1.50	-	43.5; 367	0.6	0.826; 1.682	Paddle	4	None	None	Ethyl Glycol, Water, CCl <sub>4</sub>	He; Air	(68)

TABLE III. VOLUMETRIC MASS TRANSFER COEFFICIENT, EXPERIMENTAL CORRELATIONS

Variable Correlated	Range of Experiments				Type of Correlation: Exponent of				Vessel Volume $\times 10^3$ ft <sup>3</sup>	$\frac{D^2}{T}$	T' (ft)	Impeller		Sparger		System		Reference
	$V_s$ (ft/min)	RPM	P/V (HP/ft <sup>3</sup> )	$\beta$ (%)	$\beta$	$V_s$	RPM	P/V				Type	Number of Blades	Diameter	Number	Liquid	Gas	
$k_{L,O}$	7 - 30 ft <sup>3</sup> /min	0	0	-	-	0.86 - 1.35	-	-	7	0	7	None	None	7	1	Water	Air	(19)
$k_{L,H}$	0.06 - 0.35	0	0	-	-	0.63 - 0.95	-	-	7.77	0	0.165	None	None	Aloxite Stone	20	Water + Detergents	Air	(20)
$k_{L,H}$	0.06 - 0.35	0	0	-	-	0.85 (?)	-	-	7.77	0	0.165	None	None	Nylon Spinnerette 35/4	20	Water + Detergents	Air	
$k_{L,H}$	0.033 - 0.15	0	0	-	-	0.56 - 0.80	-	-	1.24	0	0.149	None	None	Sintered Glass 3 - 150	1	Water	O <sub>2</sub>	(53)
$k_{L,H}$	0.38 - 2.66	0	0	-	-	0.82	-	-	7.06	0	0.462	None	None	1.5 mm	1	Yeast	Air	(33)
$k_{L,H}$	0.38 - 2.66	0	0	-	-	0.33	-	-	7.06	0	0.462	None	None	Fritted Stainless Steel 35/4	1	Yeast	Air	
$k_{L,H}$	0 - 12.5	0	0	0 - 38	-	0.74	-	-	2.12; 4.24; 6.48	-	{0.0825; 0.165; 0.33}	None	None	Porous Plates (Bronze; Carbon; Stainless Steel)	1	Water	{CO <sub>2</sub> ; H <sub>2</sub> ; C <sub>2</sub> H <sub>2</sub> ; SO <sub>2</sub> }	(61)
$k_{L,H}$	13 - 20	0	0	38 - 32	-	0	-	-	-	0	-	None	None	Stainless Steel	1	Water	{CO <sub>2</sub> ; H <sub>2</sub> ; C <sub>2</sub> H <sub>2</sub> ; SO <sub>2</sub> }	
$k_{L,H}$	0.11 - 5.3	0	0	1.5 - 8	-	0.98	-	-	{15.5 - 3180}	0	{0.258; 1.98}	None	None	2.25-40 mm	1	Water and Sulfite	Air and O <sub>2</sub>	(75)
$k_{L,H}$	11 - 55	0	0	12 - 40	-	0.85 - 0.31	-	-	-	0	-	None	None	2.25-40 mm	1	Water and Sulfite	Air and O <sub>2</sub>	
$k_{L,H}$	0.0182; 0.0502; 0.181	0	-	-	-	{0.59 - 0.69}	-	-	{8.4}	0	{0.5}	None	None	Fritted Glass 1/4"	1	Water	Air	This Work
$k_{L,H}$	0.33 - 11	60 - 900	$3.04 \times 10^{-4} - 9.11 \times 10^{-2}$	-	-	0.67	-	0.95	9.54; 237	0.4	0.5; 1.45	Vaned Disc	16	7	1	Sulfite	Air	(12)
$k_{L,H}$	0.75 - 3.03	100 - 1250	$3.94 \times 10^{-4} - 2.45 \times 10^{-2}$	-	-	0.67	-	0.95	38.8; 38800	0.25	0.792; 8.05	Paddle	2	7	1	Sulfite	Air	
$k_{L,H}$	0.38 - 2.34	300 - 430	-	-	-	0.68	-	-	7.07	0.38	0.462	Vaned Disc	7	1.5 mm	3	Yeast	Air	(32)
$k_{L,H}$	0.09 - 15	120 - 550	$\left\{ \begin{array}{l} N^2 \text{ ft}^2/\text{min}^3 \\ 3 \times 10^5 - 2.1 \times 10^8 \end{array} \right\}$	-	-	0.67	2.00	-	9.54; 42.4; 145	0.40	{0.50; 0.825; 1.24}	Turbine	12	8 mm	1	Sulfite Sulfate Water	{Air, O <sub>2</sub> ; O <sub>2</sub> ; Air, O <sub>2</sub> }	(76)
$k_{L,H}$	0.04 - 15	120 - 650	-	-	-	0.40 - 0.84	1.29 - 2.05	-	-	-	-	Vaned Disc	16	{4 mm}	1	Water	{Air, O <sub>2</sub> ; O <sub>2</sub> ; Air, O <sub>2</sub> }	
$k_{L,H}$	0.18 - 1.1	250 - 800	-	-	-	0 - 1	-	-	{17.7}	?	{0.50}	Turbine	7	Sintered Glass	1	Streptomycin	Air	
$k_{L,H}$	0.18 - 1.1	250 - 800	-	-	-	0 - 1	-	-	-	?	-	Turbine	7	Constricted Pipe	1	Sulfite	Air	(1)
$k_{L,H}$	0.06 - 1.1	-	0 - 0.00793	-	-	0.40	-	0.33	94000	-	10	-	-	-	-	-	-	
$k_{L,H}$	0.06 - 1.1	-	0 - 0.00793	-	-	0.40	-	0.33	$3.72 \times 10^6$	-	{0.20}	Turbine	{8}	Perforated Ring	1	Active Sludge	Air	(50)
$k_{L,H}$	0.06 - 1.1	-	0 - 0.00793	-	-	0.40	-	0.33	6.71	0.7	0.43	Turbine	8	-	-	-	-	(55)
$k_{L,H}$	0.12 - 1.1	620 - 1780	0.0045 - 0.15	-	-	0.76	-	0.71 - 0.79	49.5; 77.7; 159	0.33	0.5; 1.0	Multiple Turbine	8	7	7	Sulfite	Air	(59)
$k_{L,H}$	0.03 - 0.24	200 - 950	0 - 0.57	-	-	-	2.4 - 3.0	-	70.6	0.31 - 0.46	1.09	Turbine	4	1/4"	1	Sulfite	Air	(21)

TABLE III. VOLUMETRIC MASS TRANSFER COEFFICIENT, EXPERIMENTAL CORRELATIONS (CONTINUED)

Variable Correlated	Range of Experiments			Type of Correlation: Exponent of				Vessel Volume x 10 <sup>3</sup> (ft <sup>3</sup> )	D <sub>v</sub> /T <sub>v</sub>	T <sub>v</sub> (ft)	Impeller		Sparger		System		Reference	
	V <sub>0</sub> (ft/min)	RPM	T/V (HP/ft <sup>3</sup> )	β (%)	β	V <sub>0</sub>	RPM				T/V	Type	Number of Blades	Diameter	Number	Liquid		Gas
k <sub>L</sub> A	0 - 3.33	135 - 790	-	-	-	0.75	1.67	-	6.71	0.7	0.43	Turbine	2 (8)	Perforated Ring 0.0135"	25	o-Methyl Styrene	H <sub>2</sub>	(35)
k <sub>L</sub> E	1.33	500 - 1000	0.0275; 0.0352	-	-	C.G.H. (?)	2.00 (?)	-	10.6	0.5	0.5	Turbine	6	The Stirrer Shaft		Sulfite; Nitrobenzene	O <sub>2</sub> ; H <sub>2</sub>	(62)
k <sub>L</sub> D	0.43	600 - 4300	-	-	-	-	-	-	1.77	0.62	0.33	Turbine	8	7	1	Sulfite	Air	(56)
k <sub>L</sub> D	0.4 - 4.0	0 - 3600	-	-	-	0	1	-	7.77 - 2010	0.2 - 0.7	0.462 - 3.0	Turbine	6	Perforated Ring	1	Sulfite	CO <sub>2</sub>	(72)
k <sub>L</sub> A	0.4 - 4.0 (?)	0 - 3600	-	-	-	0	1	-	9.34 - 600	0.2 - 0.7	0.5 - 2.0	Paddle	4					
k <sub>L</sub> D	0.4 - 4.0 (?)	0 - 3600	-	-	-	0	1	-	14.0; 27.6	0.5; 0.7	0.63	Paddle	2	Porous Glass		Sulfite	Air	
k <sub>L</sub> A	0.4 - 4.0 (?)	0 - 3600	-	-	-	0	1	-	15.2 - 33.5	0.4; 0.6; 0.7	0.63	Propeller	3					
k <sub>L</sub> A	0.1 - 4.1	645 - 1990	-	-	-	0.21	2.01	-	7.07	0.5	0.33	Turbine	6	4 mm	1	Sulfite	Air	(34)
k <sub>L</sub> A	0.08 - 6.9	400 - 1600	-	-	-	0.13	2.10	-	7.07	0.5	0.33	Turbine	6	4 mm	1			
k <sub>L</sub> A	0.31 - 7.0	1200 - 3400	-	-	-	0.14	2.17	-	0.71	0.47	0.198	Vaned Disc	4	6 mm	1	Sulfite	Air	(34)
k <sub>L</sub> A	0.50 - 6.0	1130 - 2200	-	-	-	0.14	2.17	-	0.71	0.42	0.198	Turbine	4	6 mm	1			
k <sub>L</sub> A	0.11 - 4.3	800 - 3200	-	-	-	0.05	1.79	-	1.77*	0.31	0.396	Paddle	2	4 mm	1	Sulfite	Air	(35)
k <sub>L</sub> A	0.11 - 2.5	800 - 3200	-	-	-	0	1.26	-	1.77*	0.31	0.396	Paddle	4	4 mm	1			
k <sub>L</sub> A	0.16 - 14.5	300 - 2000	N <sup>3</sup> D <sup>3</sup> (1 <sup>5</sup> /min <sup>3</sup> ) 2 x 10 <sup>3</sup> - 2 x 10 <sup>6</sup>	-	-	0	3.00	-	Spherical Container 9.54	0.2 - 0.5	0.5	Paddle	4	?	1	Sulfite	Air	(35)
k <sub>L</sub> A	0 - R	-	-	-	-	-	-	-	-	0.50	0.52M	Paddle	2	8 mm	1	Sulfite	Air	(37)
k <sub>L</sub> A	0 - R	-	-	-	-	-	-	-	-	0.33	0.5; 1.28?	Paddle	2	8 mm	1			
k <sub>L</sub> A	0 - R	-	0 - 1.438	-	-	-	-	0.45 - 0.95	10.6; 141.5; 336	0.34	0.5; 1.28?	Paddle	8	8 mm	1	Sulfite	Air; CO <sub>2</sub>	(37)
k <sub>L</sub> A	0 - R	-		-	-	-	-	-	-	-	0.30	1.65	Propeller	3	Grid; Sintered Glass			
k <sub>L</sub> A	0 - R	-	-	-	-	-	-	-	-	0.24		Hoesch	7			Sulfite	Air; CO <sub>2</sub>	(37)
k <sub>L</sub> A	0 - R	-	-	-	-	-	-	-	-	0.39		Rotadux	7					
k <sub>L</sub> A	0.03 - 16.7	300 - 1080	-	-	-	0.40	1.70	-	5.3	-	0.5 (?)	Propeller	7	Perforated Ring	1	Yeast	Air	(64)
k <sub>L</sub> A	0.0182; 0.0902; 0.1M	0 - 1500	-	-	-	0.49 - 0.75	0.70 - 1.60	-	18.4	0.33	0.5	Paddle	2	Fritted Glass 1/4"	1	Water	Air	This Work

## CHAPTER III

### EXPERIMENTAL

This chapter will consist of three major parts: apparatus, materials, and experimental procedure.

#### Apparatus

The experimental apparatus consisted of the following parts:

- a. Agitated vessel with stirrer,
- b. Constant temperature bath,
- c. Dissolved oxygen analyzer, and
- d. Other auxiliary equipment.

Agitated Vessel: The agitated vessel was a 15.2 cm. (6 in.) diameter and 30.4 cm. (12 in.) high Pyrex tube. It was closed by an aluminum plate at the bottom fastened by an aluminum gasket. The vessel was baffled by four 1.7 cm. wide and 28.4 cm. high metallic baffles which were fixed to the inside walls of the container. The four baffles were equally spaced around the vessel. The top of the vessel was covered by two semicircular and removable pieces of tile. These two pieces were placed to leave a wedge-shaped opening for insertion of the oxygen analyzer probe from the side and the stirrer shaft from the center.

Two air spargers were used in the experiments in order to obtain different size bubbles. The sparger that gave the smaller bubbles was a fritted glass diffuser, and the sparger that gave the larger bubbles

was a piece of quarter-inch copper tubing. The air sparger was placed at the center of the plate closing the bottom of the vessel, and the tip of the sparger was 7.7 cm. above the bottom of the vessel.

The stirrer was a two-blade stirrer with a diameter of 5.1 cm., and was powered by a Lionel, Type CR3, variable speed electric motor. The blade was located approximately 16 cm. from the bottom of the vessel.

The agitated vessel was supported from the top by two aluminum rods, and was immersed in a 14 gallon drum, which was used as a constant temperature water bath.

Constant Temperature Bath: As mentioned above, the constant temperature bath was a 14 gallon barrel in which the agitated vessel was placed. The wall of this barrel was insulated by a layer of asbestos insulation. Water at constant temperature was introduced into the bath at a distance almost halfway down the depth of the water bath. The water left the bath from an exit at the top of the water level and 180° from the position of the inlet pipe.

Bath water was obtained from and returned to a constant temperature water source. The introduction of the constant temperature water to the bath was made possible by the use of a centrifugal pump (Precision Scientific Co., Serial No.: P-5). The water leaving the bath returned to its original source by gravity.

For the 50°C runs water was heated by an 850 watt heating unit (American Instrument Co., Serial No.: A15889) complete with a stirrer, thermostat and a water container. For the 10°C runs the water was cooled down and maintained at this temperature by a cooling unit (Blue M Electric Co., Model: PCC-1A).

Dissolved Oxygen Analyzer: The instrument used for the dissolved

oxygen measurements in water was a Beckman Model 76 Expanded Scale pH Meter, in conjunction with a Beckman 96260 Oxygen Adapter Box, and a Beckman 39065 Polarographic Oxygen Sensor, all from Beckman Instruments, Inc.

Other Auxillary Equipment: The electric motor that powered the stirrer which agitated the contents of the experimental vessel was connected to a milliammeter-voltmeter (Simpson Model 59, Simpson Electric Co.) combination, which was in turn connected to a Variac.

A stroboscope (Model 510-AL; Electronic Brazing Co.) was used to measure the stirrer speeds.

The air that was used in the experiments as the source of oxygen was obtained from the laboratory air line. The air first passed through a pressure regulator (Air Reduction Co., Oxygen 8950, Serial No.: 27-2748), and then through an air drier (Drierite). Two thick cloth filters were used at the entrance and exit of the drier to hinder the passage of impurities. The dry air that left the drier then passed through a regulating valve, a rising soap film flowmeter, a rotameter (The Matheson Co., No.: 603), and then finally through the air sparger in the agitated vessel. The air line was made of quarter-inch copper tubing, and passed through the constant temperature bath before reaching the sparger, in order to bring the temperature of the air to the temperature of the bath.

The pressure on the nitrogen purge gas was controlled by a two-stage pressure regulator (Air Reduction Co., Gauge No.: 8410003, and Gauge No.: 8410102).

The barometer used in measuring the atmospheric pressure was available in the Chemical Engineering building.

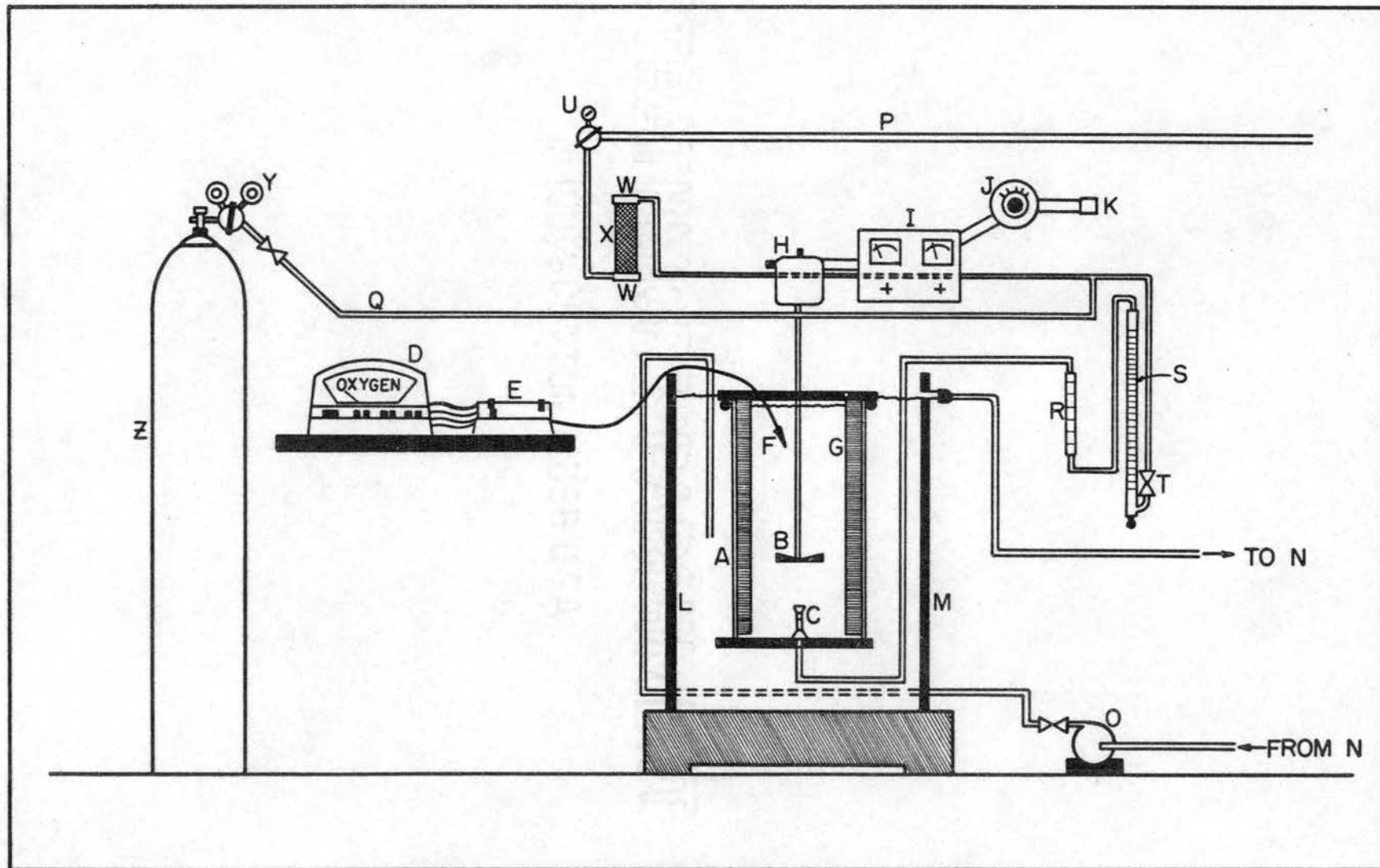


Figure 1: EXPERIMENTAL APPARATUS

Listing of the Experimental Apparatus

(From Figure 1)

- A - Agitated vessel
- B - Impeller
- C - Sparger
- D - pH meter
- E - Oxygen adapter box
- F - Oxygen sensor
- G - Baffles
- H - Electric motor for the agitator
- I - Voltmeter-ammeter combination
- J - Variac
- K - Electric outlet
- L - Constant temperature bath
- M - Insulation
- N - Constant temperature water source
- O - Pump
- P - Air line
- Q - Nitrogen line
- R - Rotameter
- S - Rising soap film flowmeter
- T - Flow regulating valve
- U - Air pressure regulator
- W - Air drier
- X - Filters
- Y - Nitrogen pressure regulator
- Z - Nitrogen gas bottle



A stopwatch was used to measure the aeration time intervals, and a mercury thermometer was used for the temperature measurements.

Conventional laboratory glassware, and an analytical balance were used in the Winkler (azide modification) analysis for the dissolved oxygen.

### Materials

The materials used for the experiments were as follows:

- a. Water,
- b. Air,
- c. Nitrogen gas,
- d. Plastic (Polystyrene), and
- e. Chemicals for the Winkler (azide modification) analysis.

Water used for the experiments was tap water filtered through the bed of the water de-ionizer, available in the School of Chemical Engineering.

Air was obtained from the compressed air line available in the laboratory.

Nitrogen gas was obtained from commercial cylinders.

The plastic particles that were used in some of the experimental runs were made of OSS 44974 Polystyrene, supplied free of charge by the Phillips Petroleum Company, Bartlesville, Oklahoma.

The chemicals used in the Winkler determination were reagent grade chemicals. Distilled water was used for solutions of these chemicals.

### Experimental Procedure

The experimental procedure is summarized as follows:

- a. The constant temperature bath was brought to the proper temperature for the run.
- b. Water was put into the experimental vessel and brought to the desired temperature.
- c. Nitrogen gas was passed through the water in the vessel to drive out the dissolved oxygen.
- d. The stirrer was brought to the desired speed, as measured by the stroboscope.
- e. Air, at the proper flow rate, was introduced into the de-oxygenated water through the sparger.
- f. The aeration intervals were measured by a stopwatch, and the oxygen concentration of the water was measured by the oxygen meter.

Following the outline of the experimental procedure, the steps will now be explained in more detail.

Adjustment of the Constant Temperature Bath: The correct setting of the temperature controller was found by trial and error. This procedure seemed to be quite satisfactory since once the desired temperature was obtained a series of runs were made at this temperature. The temperature controller settings controlled the temperature satisfactorily for the purposes of these experiments at  $\pm 0.5^{\circ}\text{C}$ .

Driving the Dissolved Oxygen Out of the Water: After the experimental water was brought to the temperature at which it would be maintained all through the experiment, the nitrogen gas was introduced into the water from the sparger, and the contents of the vessel were well agitated by the stirrer, running at about 1000 rpm. Thus, by passing

the nitrogen gas through the agitated liquid for a sufficient amount of time,<sup>\*</sup> the dissolved oxygen content of the experimental water was reduced to a low enough level to give a reasonably good starting point for the experiment.<sup>\*\*</sup>

Adjustment of the Stirrer Speed: While the water in the agitated vessel was being de-oxygenated by nitrogen, the speed of the stirrer was brought to the desired value for that particular run. The experimental runs were made at stirrer speeds of 0, 250, 600, 1000, and 1500 revolutions per minute. The speed of the stirrer was controlled by changing the input voltage from a Variac. The revolutions per minute at the lowest speed, i.e. 250 rpm., were determined by hand contact with the set screw on the chuck of the stirrer. The desired count was fifty contacts of the set screw in a twelve second time interval. As with all other revolution measurements, this was repeated at least three times for accuracy. This type of measurement is believed to be correct up to

---

<sup>\*</sup> During the trial runs made before the start of the actual experiments, two methods for the de-gassing (de-oxygenation) of water were tried. The one given above was found to be a much better way for the purposes of this study, and it was adopted. The abandoned method was as follows: Water was boiled for about half an hour to forty-five minutes in a large Erlenmeyer flask. Then the boiling was discontinued and the flask was fitted at the mouth with a rubber stopper which had an inlet hole for the nitrogen purge gas and a very small exit hole. Then the flask was put into a cooling bath and the nitrogen gas was turned on. After the water was cooled down to about room temperature it was siphoned into the experimental vessel, covered at the top, and nitrogen was passed through it until it attained the desired temperature.

This procedure consumed more time and effort than the adopted process and did not give superior results; therefore its practice was discontinued.

<sup>\*\*</sup> From the above discussion it should be understood that when de-oxygenated in this way, the dissolved oxygen concentration of the experimental water at the start of the experiments was not always necessarily the same.

+10 revolutions per minute at 250 rpm. At higher speeds the stroboscope, was used for the determination of the stirrer speed. At all runs where the stirrer speed was measured by the stroboscope, the direct reading of the low scale of the instrument was used, and for all readings the stroboscope was calibrated at its low scale.

After the de-oxygenated water had attained its desired temperature and agitation, it was aerated by passing through it a measured quantity of air for a recorded length of time.

Calibration of the Flowmeter: Two flowmeters were used in the experimental apparatus (Figure 1) to measure the air used in aerating the water. The flowmeters, a rising soap film flowmeter and a rotameter, were connected in series on the air line, the rotameter being nearer to the air regulator. The rising soap film flowmeter was used for the determination of the rotameter reading for a given flow rate. Prior to a new set of runs with a different air flow rate, and/or with a different sparger, and/or with a different temperature, the rotameter was calibrated with respect to the rising soap film flowmeter in the following manner: The pressure regulator on the pressurized air line was manipulated until it showed a pressure of five pounds per square inch,<sup>\*</sup> and then the regulating valve at the inlet of the rising soap film flowmeter was opened, thus letting air to flow through the remainder of the system. During the rotameter calibrations the amount of water (i.e., the water level) in the experimental vessel was kept constant to keep a constant pressure drop. During these calibrations the stirrer speed was always between 600 to 800 rpm.

---

\*This was the gauge pressure used for all of the experimental runs.

The flow rate of the air flowing through the system was measured by timing the rise of a single soap film for a volume of one hundred cubic centimeters in the rising soap film flowmeter. This initial flow rate was then increased or decreased by adjusting the valve until the desired flow rate was attained. After the desired air flow rate was achieved, the reading of the stainless steel ball (the bottom of the ball) of the rotameter was read and the reading was recorded. After this first reading was taken the air was turned off, and then the valve was opened again until the reading of the rotameter was the same as before. While the air was flowing at this setting, its volumetric flow rate was measured again by the rising soap film flowmeter. At all times these two consecutive readings were checked against each other. The experiments were made at three different air flow rates: 100, 500, and 1000 cc./min.; corresponding to 0.55, 2.73, and 5.47 cm./min. superficial gas velocities, respectively.

Timing the Aeration: While the water was being de-oxygenated, the probe of the oxygen analyzer was put into the water, and the de-oxygenation was continued until the reading of the oxygen meter was below a partial pressure reading of ten millimeters of mercury. When this reading was attained, the flow of the nitrogen gas through the system was discontinued by closing the pressure regulator on the nitrogen bottle. The regulating valve at the entrance of the rising soap film flowmeter was not closed at this moment and the pressurized nitrogen gas remaining in the lines was allowed to bubble out until it stopped. Then the regulator valve was closed and the air line pressure regulator was turned on until five psig. was read on the indicator of the regulator. This was followed by the first measurement of the dissolved

oxygen concentration of the water (i.e., at time equal to zero). Following this initial measurement, the valve on the air line was opened until the steel ball of the rotameter rose up to the desired and predetermined (see 'Calibration of the Flowmeter') reading.\* At this moment the stopwatch was started. After a short time interval the air was turned off, the stopwatch stopped, and another reading of the dissolved oxygen concentration of the water was made by the oxygen analyzer.\*\* Following this, air was turned on again, the water was aerated for another determined length of time, another oxygen concentration was measured, etc. The aeration time intervals were relatively much shorter during the initial phases of the total aeration period than they were during the later part. The first few intervals were usually between half a minute and one minute. The aeration intervals were increased gradually. The longest intervals were about twenty minutes each, for the runs with low flow rates and low agitator speeds.

In the previous explanation on the aeration time it was mentioned that the air flow was stopped while dissolved oxygen measurements were taken. This interruption was made for the reason that, had it not been done, then the indicator needle would have shifted continuously due to the incoming new air. It is hoped that in the future

---

\* By experience it became possible to quickly attain the rotameter reading that would give the desired air flow rate.

\*\* During the 100 cc./min. runs it was noticed that for the first minute of the air flow the oxygen concentration of water would, usually, very slightly decrease. This was believed to be due to the nitrogen gas that had remained in the lines, and being pushed out by the incoming air. Thus, for these runs, the initial oxygen concentration measurement was made after the first minute of the gas flow after the air was turned on. For the runs with 500 and 1000 cc./min. this was not necessary.

this drawback could be evaded, and continuous oxygen determinations could be made.

Calibration of the Dissolved Oxygen Analyzer: It was mentioned above that a Beckman oxygen analyzer was used to determine the concentration of the dissolved oxygen in the water. The partial pressures of the dissolved oxygen were measured, and these partial pressure measurements were recorded. However, calculations were done with oxygen concentrations as expressed in parts per million (ppm. oxygen in water). Thus, it was necessary to know the dissolved oxygen concentration in parts per million corresponding to the partial pressure readings of the oxygen analyzer. These conversions were accomplished by the use of a prepared calibration chart (see Appendix A). Since the oxygen solubility changes with temperature, the meter was calibrated for each of the temperatures at which experiments were made.

This type of calibration is called the "grab sample method" by the Beckman Bulletin (4), and was performed as follows: The meter was first calibrated with respect to air (see the following 'air calibration' method) and then the oxygen analyzer probe was put into the water in the experimental vessel and the partial pressure reading of the dissolved oxygen was taken. Immediately after this reading, a sample was taken from the water in the vessel and it was analyzed with the Winkler (Azide Modification) Method (63). The Winkler gave the dissolved oxygen concentration in parts per million. The dissolved oxygen concentration was changed according to need by passing either air or nitrogen through it. In this manner a wide range of oxygen concentrations were covered. The results of this calibration gave a graph of partial pressure versus parts per million of dissolved oxygen in water, at a

constant temperature (Appendix A).

Another type of calibration procedure, i.e., air calibration (4), was performed to ensure that the same basis was taken for all readings in all of the runs. The meter was calibrated prior to every run by this method. The procedure of the 'air calibration' was as follows: The atmospheric pressure was measured by a barometer and this value (in millimeters) was multiplied by 0.21<sup>\*</sup> to get the partial pressure of oxygen in air. This value of the partial pressure of oxygen in air was the value for the dissolved oxygen in water when the water was 100% saturated with oxygen.<sup>\*\*</sup> Next, the range control selector on the oxygen adapter box was put on zero. The zero calibration dial, also on the adapter box, was used to zero the indicator needle on the pH meter. The range control selector was then turned to the 0-250 mm. position (for all experiments this was the only range used) and the sensor was moved back and forth in air. After the indicator needle steadied, i.e., indicated only one point (no drift), it was set at the precalculated value of the oxygen partial pressure in air using the calibration dial, also on the adapter box.

Dissolved Oxygen Concentration Measurements: As was mentioned, the partial pressure of the dissolved oxygen in water was determined by the Beckman Oxygen Analyzer, using the 0-250 mm. scale, after the meter was calibrated with respect to air.

In the Beckman instruction booklet (3) for the oxygen analyzer it

---

\* Air is about twenty-one mole per cent oxygen.

\*\* This is because of the fact that at 100% saturation the partial pressure of the dissolved gas should be equal to its partial pressure in the gas mixture above the liquid.



was noted that some oxygen should be consumed by the probe during the process of measurement due to the polarographic reaction. For this reason, the booklet stated that the measured media should be passing the probe with a minimum of 1.5 ft./sec. Because of this, the probe was moved back and forth in the water while a reading was being taken. At 0 and 250 rpm. runs the indicator needle of the oxygen meter shifted considerably with this movement. In these cases the reading at which the needle became stationary was recorded. At agitator speeds of 600 rpm. and higher this shifting due to the motion of the probe was almost unnoticeable. The data recorded for these runs were based on the indicator readings after the shifting had ceased. Another reason for moving the probe in the explained manner during a measurement was to hinder any possibility of an air bubble being trapped on the sensing part of the probe. Appendix C includes some data taken to test the reproducibility of the readings. This was done because in some cases it was a matter of judgement to decide whether the indicator was stationary or whether it was moving very slowly.

Preparation of the Plastic Particles: The plastic particles that were used in some of the experiments were made of polystyrene (Phillips Petroleum Co.) which had a specific gravity of 1.03. The method was to shape the supplied small granules into cylinders of 3/16 inches in diameter and 1/4 inches in height by forming them in a specially prepared mold. This mold consisted of two flat aluminum slabs with the proper sized holes. After the melted polystyrene filled the molds, the molds were taken off the hot plate and cooled. After the cooling the polystyrene particles were pushed out of the holes in the mold.

Experiments With Particles in the Agitated Vessel: The runs that

were made in the presence of the plastic particles followed exactly the same procedure as that described for the other runs. The only difference was that the particles were put into the water. There were one hundred and thirty five particles. Their diameters were 0.45 cm.  $\pm 0.1$  cm. and lengths were 0.5  $\pm 0.1$  cm. The specific gravity of the particles were such that with no agitation almost all of them would be at the bottom of the vessel, but at 600 rpm. almost all would be moving around.

Approximate Measurement of the Bubble Size: The bubble size range involved in the experiments was determined by an approximate comparison method, i.e., comparing the bubble size with objects of known sizes placed into the vessel. For this reason the agitated vessel had to be taken out of the constant temperature bath. The size determination was done at the ambient conditions (Appendix E).

Effect of the Surface Aeration: Effect of the surface aeration was determined with no stirring, and with an rpm of about 1000. The procedure was to measure the oxygen concentration in the water at different intervals, with and without the stirrer running, all the other conditions being constant, and at zero air rate through the sparger. The results are given in Appendix F.

## CHAPTER IV

### DISCUSSION OF RESULTS

Raw data consisted of oxygen concentrations in water as measured by the oxygen analyzer at different times during a run. A representative sample of this data is shown together with a sample calculation for the  $k_L a$  determination in Appendix B. The  $k_L a$  values obtained from the experiments are tabulated in Appendix D. The  $k_L a$  values were plotted versus their corresponding power factor ( $N^3 D^2$ ), Reynolds number, stirrer speed, superficial gas velocity, and temperature. From these plots a correlation was obtained giving  $k_L a$  as a function of the above listed variables. These plots and related discussions are presented below. In addition, one of the goals of this study was to find the effect of solid particles on  $k_L a$ . The first parts of this chapter will be devoted to the discussion of the results of the runs where a stirrer was employed; these will be followed by a discussion of the case where there was no mechanical agitation.

#### $k_L a$ as a Function of $N^3 D^2$ , $N_{Re}$ , and $N$

The experimental  $k_L a$  values were plotted versus  $N^3 D^2$ ,  $N_{Re}$ , and also versus  $N$  itself. Representative plots are presented on Figures 2, 3, and 4. These plots are for a constant temperature, and each line is for a constant superficial velocity. Furthermore, as can be seen from the given figures (for the given temperature, flow rate, and impeller

speed) four different kinds of runs were made:

- a. Small Bubbles - Without Particles (SBNP)
- b. Large Bubbles - Without Particles (LBNP)
- c. Small Bubbles - With Particles (SBWP)
- d. Large Bubbles - With Particles (LBWP).

When compared, Figures 2, 3, and 4, look alike due to the evident fact that both  $N_{Re}$  and  $N^3D^2$  are functions of  $N$ . There are a few points in these plots that should be brought forward. First of all, as would be expected, at low impeller speeds the  $k_L a$  for the large bubbles is very much lower than the  $k_L a$  of the corresponding runs using the fine bubble sparger (small bubbles). This fact can be explained by the transfer area to gas volume ratio of the gas in the two cases. This point may not easily be the only factor involved in this phenomena, since  $k_L$ , too, is dependent on the liquid turbulence (7, 8, 14, 76), and different  $k_L$  values have been found for different bubble size ranges (11). This difference in the  $k_L a$ 's for the two bubble sizes studied seems to decrease and in many cases it almost converges to one  $k_L a$  value at the highest impeller speed studied. This is due to the effect of the intense agitation, as was also noticed by Karwat (37). At this point of intense agitation it seems as if the large bubbles were broken into the size of the bubbles produced by the fine bubble sparger under similar conditions. This breaking phenomena evidently increases the transfer area (see the bubble size data in Appendix E).

When the  $k_L a$ 's for different runs were plotted against their respective  $N^3D^2$  values on log-log paper it was noticed that the points corresponding to 600, 1000 and 1500 rpm. values were almost a straight line for all superficial velocities in the case of the large bubbles.

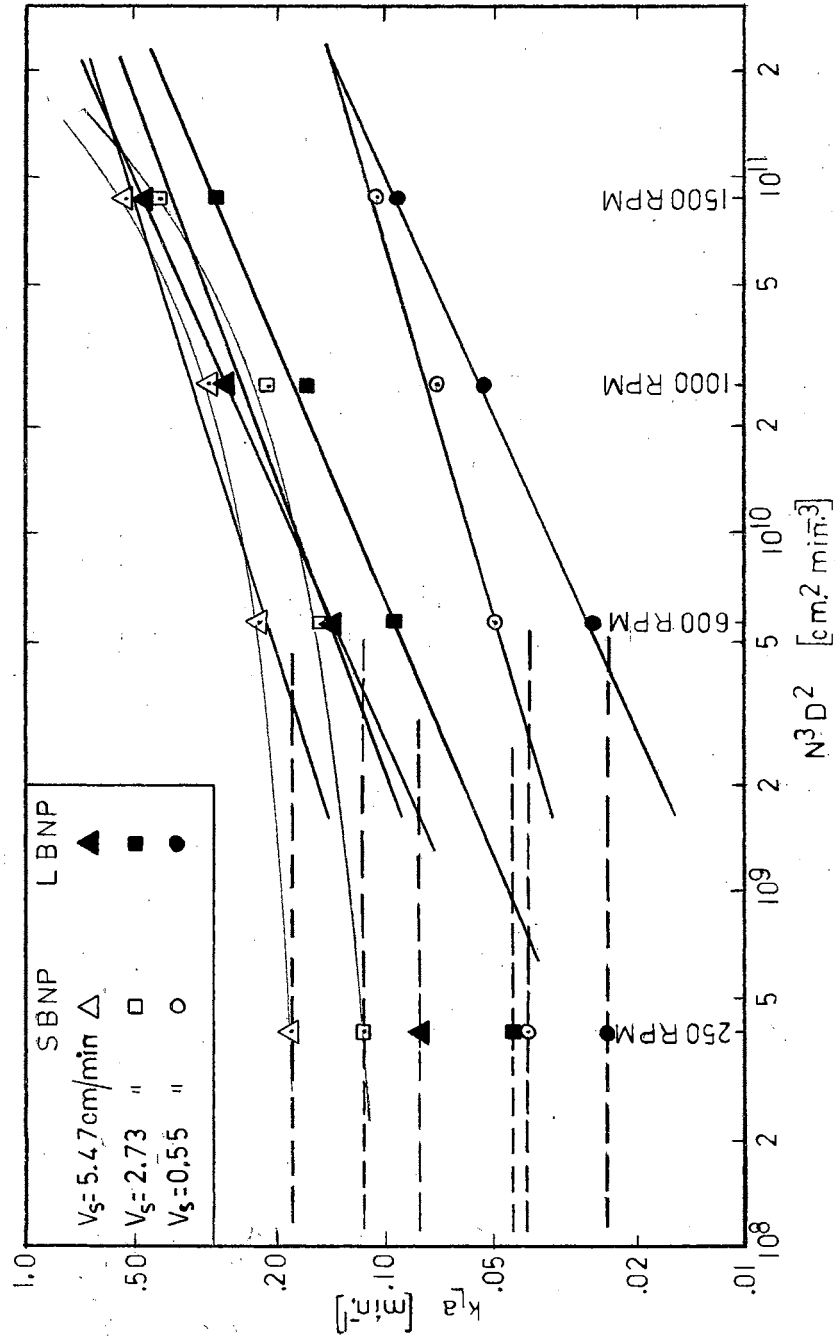


FIGURE 2. EFFECT OF MECHANICAL AGITATION ON  $k_{La}$ ;  $T=10^\circ\text{C}$ .

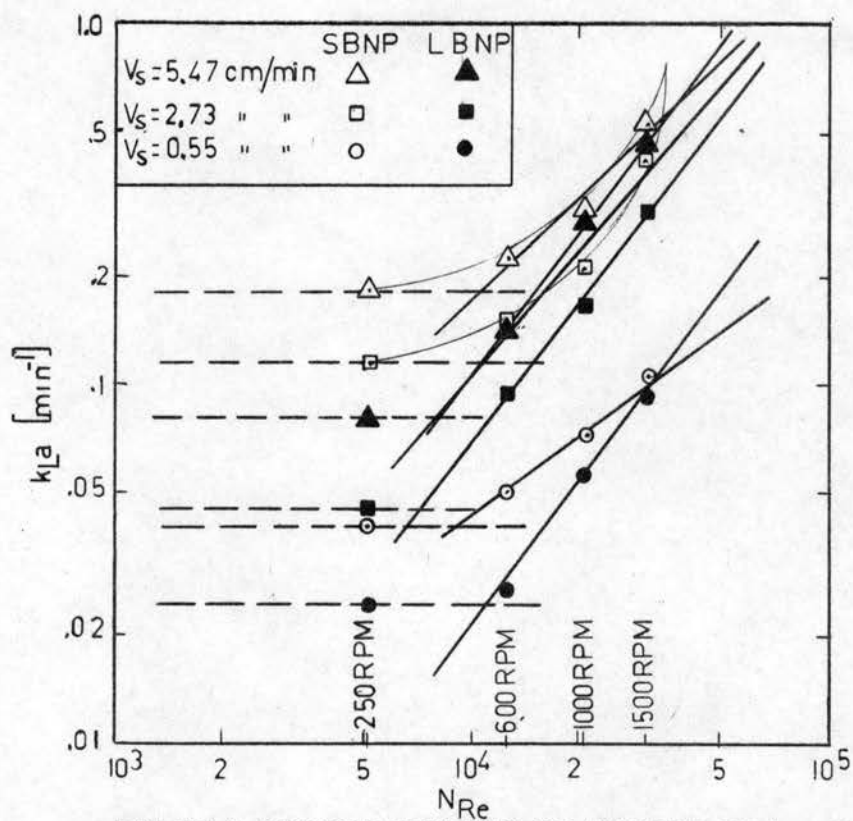


FIGURE 3. EFFECT OF REYNOLDS NUMBER ON  $k_{La}$ ;  $T=10^\circ\text{C}$

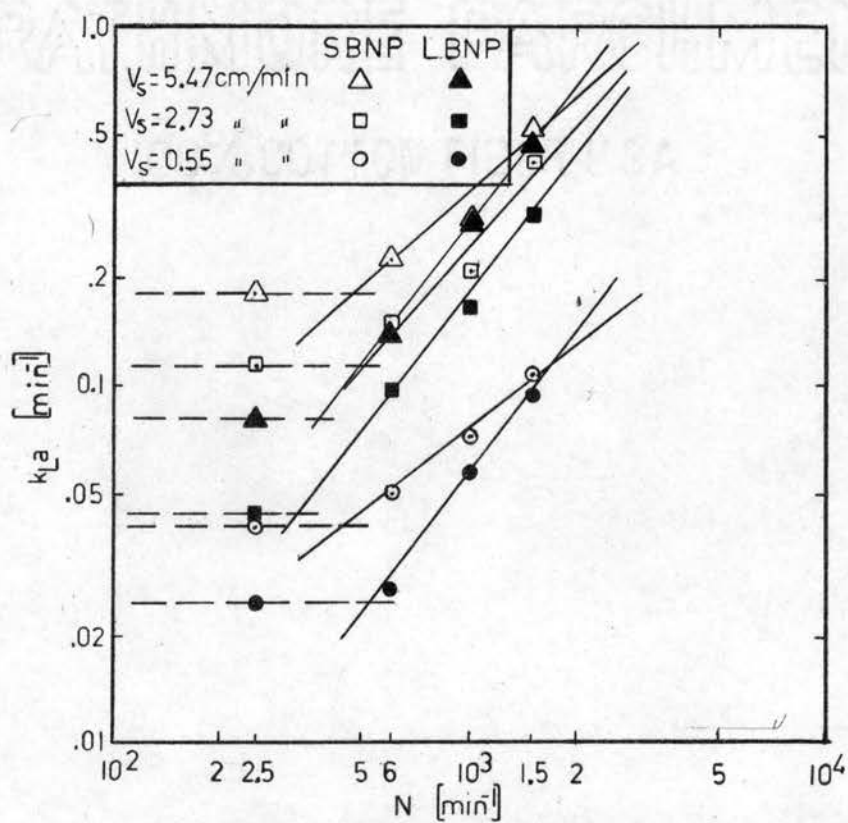


FIGURE 4. EFFECT OF AGITATOR SPEED ON  $k_{La}$ ;  $T=10^\circ\text{C}$

For the small bubbles this 'almost' straight line relationship was noticed only for the lowest  $V_s$ , and for the higher superficial velocities the line tended to curve up. Previous workers (12, 21, 25, 34, 36, 44, 62, 76, 77) have usually passed a straight line through these plots ( $\log k_L a$  vs.  $\log N^3 D^2$ ,  $\log P/V$  or  $\log N^3 D^2$ ) to get the dependence on the agitation rate. For this purpose a straight line was passed through the points to get the agitation effect on the  $k_L a$  in this work, too, using the linear regression technique. The slopes of these lines are reported in Appendix G. As can be seen, these slopes are not the same for each case. Former workers have reported either constant and/or varying dependencies for similar experiments (12, 21, 25, 34, 36, 44, 72, 76, 77). In the literature the dependency on  $N$  has been reported to be between 1 and 3 by various authors. Cooper, et al., (12) have given the  $k_L a$  dependency on  $P/V$  to be 0.95. Since  $P/V = C(N^3 D^2)$ , the proportionality constant  $C$  could well be different for the different gas loads, thus accounting for the rather high exponent value. Karwat (37) had a range of dependencies for  $P/V$ , the upper limit being 0.95. The slopes obtained from this work varied between different experiments, as was the case in some other works, but they did not show a trend as did Yoshida, et al., (76) work with vaned disc impellers.

The reason for the phenomenon of the  $\log k_L a$  versus  $\log N^3 D^2$  lines for different  $V_s$ 's converging at high agitation rates could be explained in two different ways. One explanation could be that the surface aeration has a predominant effect at these high agitation rates. The other explanation could be that above a critical agitation rate  $k_L a$  is independent of  $V_s$  but dependent only on the rpm. of the stirrer. This was proposed by Friedman and Lightfoot (25), Westerterp (72) and by

Elsworth, et al., (21). Westerterp and his co-workers stated that for each system there is a critical stirrer speed,  $n_o$ , above which  $k_L a$  is a linear function of the stirrer speed only. They also found that the superficial velocity affects neither the intercept nor the slope of this straight line. This independence of  $k_L a$  from  $V_s$ , they claimed, was due to the fact in this region of high turbulence "the gas volumes in the dispersion circulate much more rapidly than fresh gas supplied." A set of plots to this effect from the present data is given on Figure 5. It can be seen from this graph that the slopes of the lines for the two higher gas flow rates are almost equal, although the points do not fall on the same line. The points for the lowest  $V_s$  fall on another curve with a tangent which has a slope much less than the others. Now, it can be argued that the lines tend to converge at even higher stirrer speeds, but this will be very high. Since the range of this work is up to 1500 rpm., whereas Westerterp, et al., (72) had a range up to 3600 rpm., and the highest superficial gas velocity of this work corresponds to the lowest of their range (72), the phenomena proposed by Westerterp, et al. may not be valid in the range of this present work. Thus, it may now be concluded that the reason for the above mentioned convergence phenomena encountered in this work for the two higher gas rates is due to the intense agitation at the high stirrer speeds, since it was found that even at high stirrer speeds the surface aeration did not contribute appreciably to the  $k_L a$  (Appendix F). The  $n_o$  value for the highest flow rate was calculated for this work was calculated from Westerterp, et al., equation and it was found to be 1440 rpm. This number seems to be a very high prediction since as can be seen from Figures 2, 3, 4, and 5 stirring had an effect on  $k_L a$  even at lower



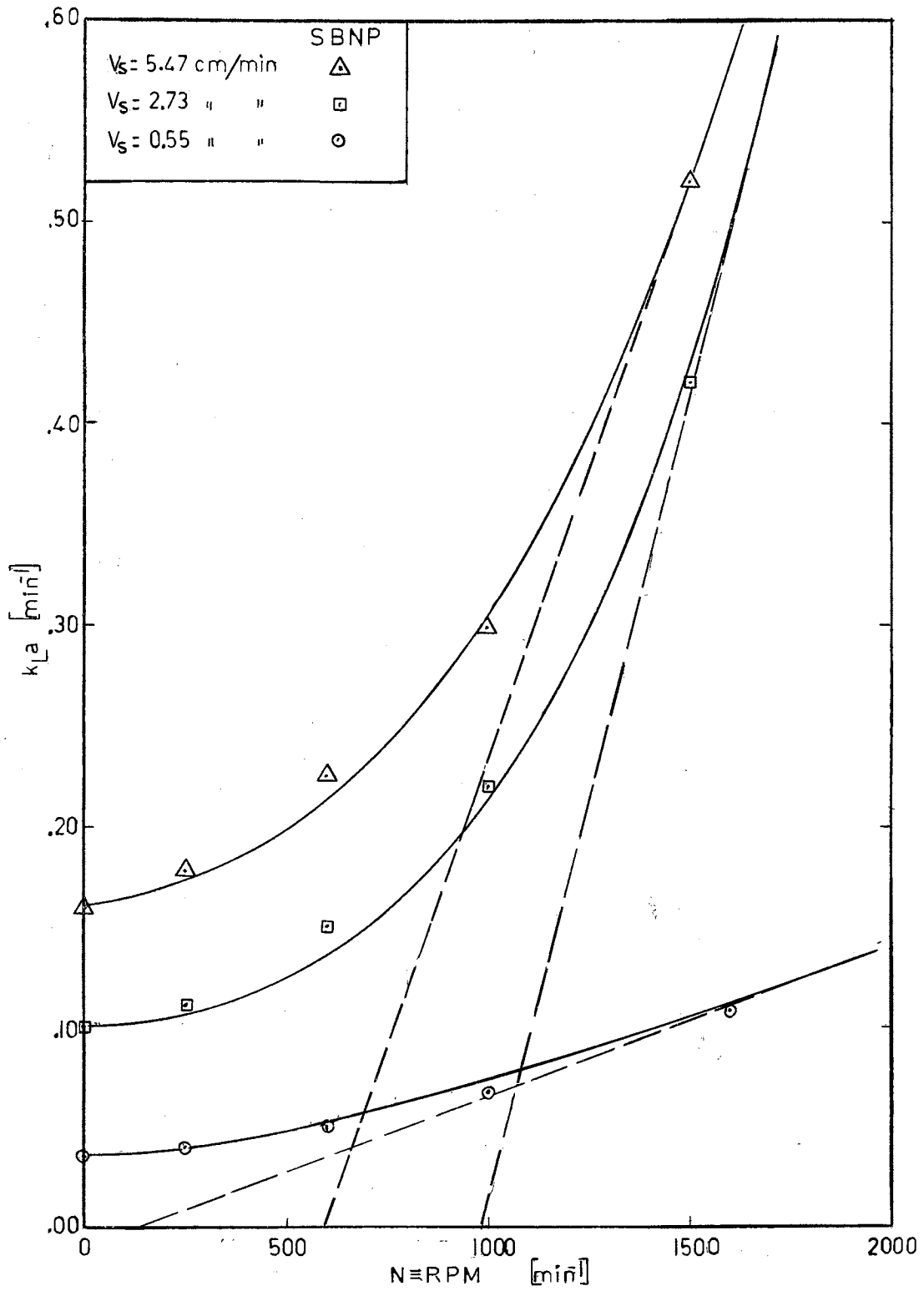


FIGURE 5. EFFECT OF STIRRER SPEED ON  $k_{La}$  ;  $T = 10^\circ\text{C}$

stirrer speeds.

The slopes for the  $\log k_L a$  versus  $\log N^3 D^2$  plots ranged from 0.22 to 0.55 in this work, with an average value of 0.37. These, if converted to dependency on  $N$  alone give 0.66, 1.11, and 1.65, respectively. The exponents given in the literature for  $N$  range from 1.26 to 3.00. Therefore one can write

$$k_L a = (N^3 D^2)^{0.37} f(V_s, T) \quad \text{IV-1}$$

where 0.37 is the average slope of the lines mentioned above. The low value of the exponent, when compared with the literature values, may be explained by the assumption that the impeller used in this work was unable to attain perfect mixing. On the other hand if one considers that Hyman and Van den Bogaerde (34) obtained a 1.26 dependency on the  $N$  with a four bladed paddle impeller, and also that Westerterp, et al., (72) claim that a four bladed paddle impeller produces twice the interfacial area as a two bladed one, it can be seen that the dependency found in this work is not excessively low.

As can be seen from the reported data and the sample plots (Figures 6 and 7), the solid particles that were added to the agitated vessel do not seem to have affected the turbulence in the vessel. Also, they do not seem to have broken the bubbles. It is evident that had either or both of these happened, the interfacial area for a given  $V_s$  and stirrer speed would have been greater, thus resulting in a  $k_L a$  higher than the one obtained for a corresponding run without the particles.

As was mentioned before, the dependence of  $k_L a$  on  $N_{Re}$ , and on  $N$  is very similar to its dependence on  $N^3 D^2$ . The reason for this type of dependence is explainable, as before, by the fact that both  $N_{Re}$ , and  $N^3 D^2$  are functions of  $N$ . The  $\log k_L a$  versus  $\log N_{Re}$  plots gave the

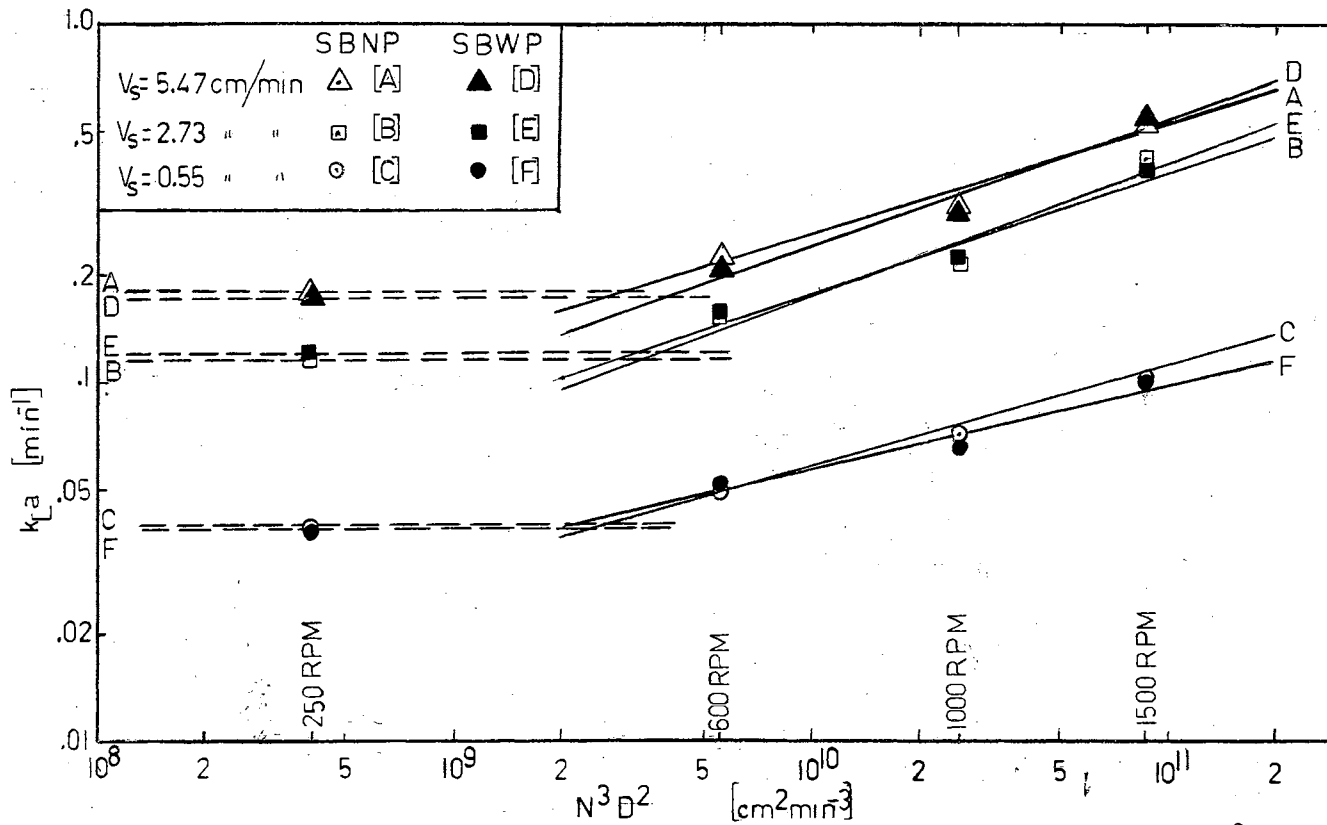


FIGURE 6. EFFECT OF SOLID PARTICLES ON  $k_{L,a}$ 's OF SMALL BUBBLES;  $T=10^\circ\text{C}$

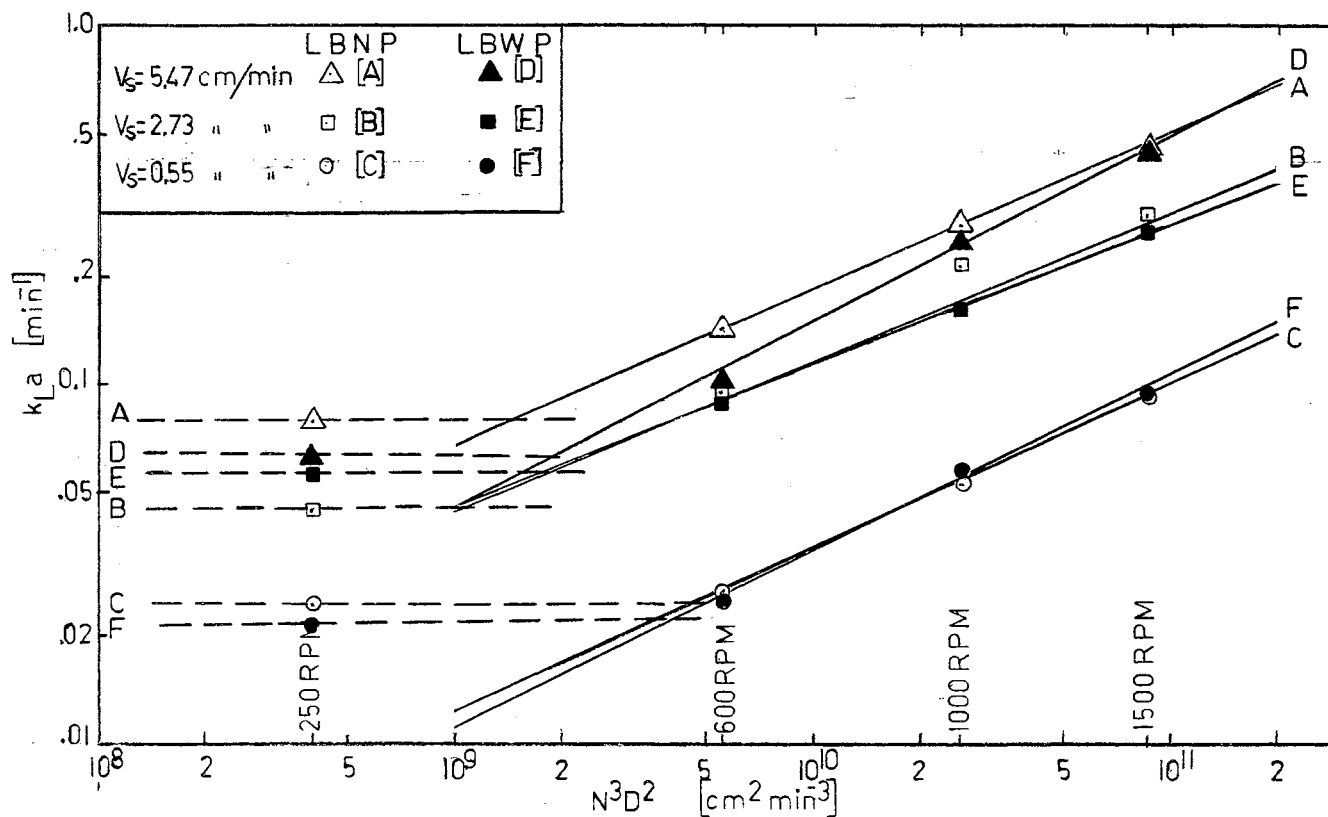


FIGURE 7. EFFECT OF SOLID PARTICLES ON  $k_{La}$ 's OF LARGE BUBBLES;  $T=10^\circ\text{C}$

following correlation:

$$k_L a = (N_{Re})^{1.12} f(V_s, T) \quad \text{IV-2}$$

where the slopes of the lines ranged from 0.66 to 1.66 with an average value of 1.12.

$k_L a$  as a Function of  $V_s$

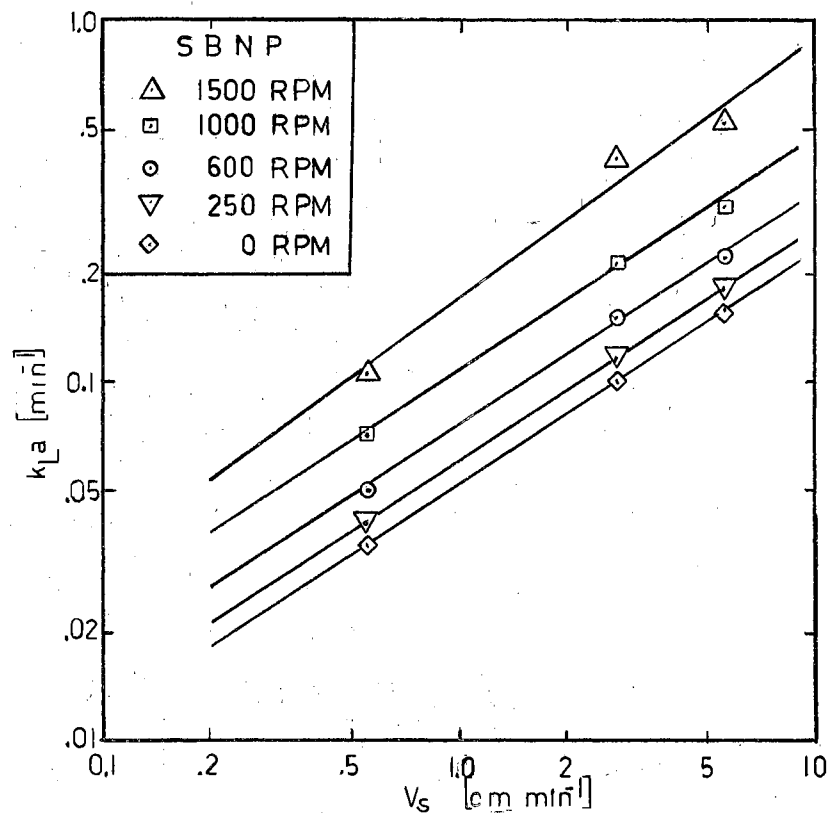
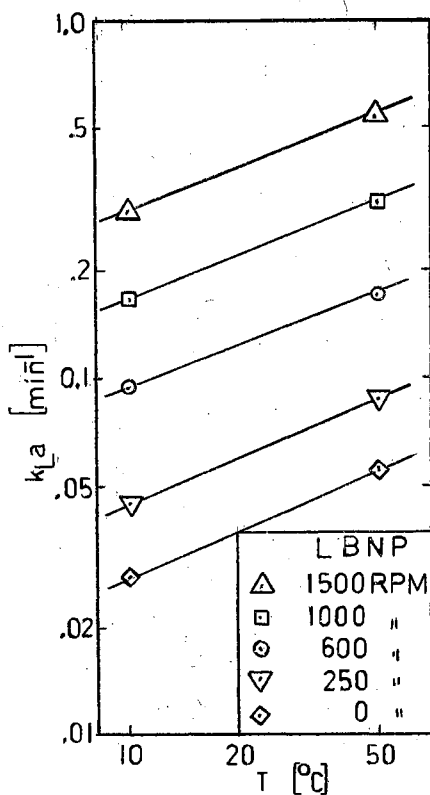
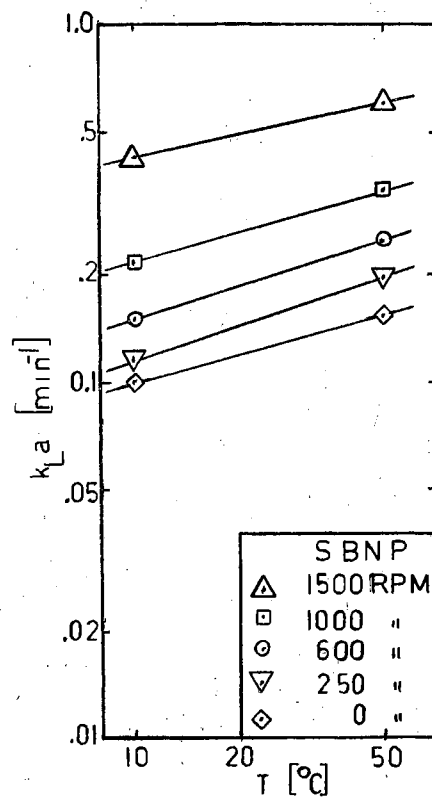
$k_L a$  versus  $V_s$  plots on log-log paper can be seen in Figure 8. Straight lines were passed through the data using the least squares technique for each rpm., and the slopes of these lines, (i.e., the exponents of  $V_s$ ), were found. The results of these calculations have shown that the exponent of  $V_s$  varies between 0.49 and 0.75, with an average value of 0.67 (Appendix H), giving the correlation

$$k_L a = V_s^{0.67} f(N, T) \quad \text{IV-3}$$

The average value of the exponent, i.e., 0.67, is identical with the values of Cooper, et al., (12), Yoshida, et al., (76, 77) (for the turbine impeller), Snyder, Hagerty and Molstad (62), and Hixson and Gaden (33). Other values reported in the literature vary between 0 and 1. The dependency of zero (0) was reported by Friedman and Lightfoot (25), Elsworth, et al., (21), and Westerterp, et al., (72) for the region of intense agitation, and the exponent of one (1) was reported by Bartholomew, et al., (1) and also by Polejes (55). The 0.67 value obtained from the present data, besides agreeing with the previously reported values, did not deviate much for all the experiments (7.7%). This deviation was much less than the deviation encountered in the  $N^3 D^2$  exponent (22.1%).

$k_L a$  as a Function of T

Figures 9, and 10 show a representative group of  $k_L a$  versus T plots

FIGURE 8. EFFECT OF  $V_s$  ON  $k_{La}$ ;  $T=10^\circ\text{C}$ FIGURE 9. EFFECT OF  $T$  ON  $k_{La}$ ; LBNP;  $V_s=2.73 \text{ cm/min}$ FIGURE 10. EFFECT OF  $T$  ON  $k_{La}$ ; SBNP;  $V_s=2.73 \text{ cm/min}$

on log-log paper. Since the experiments were made at only two different temperatures straight lines were passed through the two points available for each case and their slopes were found. It is granted that this procedure of using only two points to determine a line is questionable, but the results came out as would be expected, (i.e.,  $k_L a$  values for 10°C were lower than the ones for 50°C). The exponent of the temperature, (i.e., the slopes of these lines), ranged from 0.26 to 0.46, with an average value of 0.34 (Appendix I). The deviation from the average value is 16.1%. It will be noted that the general trend in the literature is for higher  $k_L a$ 's at higher temperatures due to the increase in the diffusivity, which in some cases is offset by the changes in the physical properties of the liquid thus changing the interfacial area (72, 76). From the results obtained one can then write,

$$k_L a = T^{0.34} f(N, V_s) \quad \text{IV-4}$$

#### Transition Point in the $\log k_L a$ Versus $\log N^3 D^2$ Plots

When the  $k_L a$  values were plotted versus their corresponding  $N^3 D^2$  values, for a constant superficial gas velocity on log-log paper (Figure 2), it was noticed that the points corresponding to the 600, 1000, and 1500 rpm. values fitted together on a straight line better than the  $k_L a$  for the 250 rpm. point. This type of behavior was also reported by Yoshida, et al., (76, 77) and can be deduced from Westerterp, et al., (72). Yoshida drew a straight horizontal line for this region passing through the  $k_L a$  value for this low rpm. In his case this line intersected the positively sloped line passing through the remainder of the points. The corresponding  $N^3 D^2$  value for this intersection has a very similar meaning to the  $n_o$  rpm. as proposed by Westerterp, et al.,

(72). Furthermore this region of transition is in fact a region, but here it is represented as a point for simplicity. This point indicates the agitation rate which is approximately the point where the mechanical agitation begins to have an effect. In the plots obtained from our data it was noticed that this point of intersection shifted to the right (i. e., to higher  $N^3D^2$ s) with increasing superficial gas velocities. Thus, if these intersection points are represented by a straight line, the line would have a very high positive slope rather than being perpendicular to the horizontal axis. This is not unusual since the same thing occurs for the case of no mechanical agitation, as discussed later and as obtained in different ways by Calderbank and Moo-Young (9) and Karwat (37). The similarity between the two is that in the case of no mechanical agitation (i.e., air agitation only) all of the agitation is due to the gas. Up to the transition point the gas agitation is the predominant one.

The above discussion leads one to conclude that the transition region could be correlated as a function of the gas flow rate and mechanical agitation rate if enough data were available. The same transition phenomenon is expected from the  $\log k_L a$  vs.  $\log N_{Re}$ , and  $\log N$  plots.

Dependence of  $k_L a$  on  $N^3D^2$ , and on  $V_s$  in  
the Absence of Mechanical Agitation

In Figure 5 it is seen that as the stirring rate is decreased, especially for speeds lower than 250 rpm., the curve becomes asymptotic to a horizontal line. The same behavior was also noticed in the  $\log k_L a$  vs.  $\log N^3D^2$  plots. This behavior leads to the idea of utilizing a



graphical method with which one can find the approximate and relative agitation rate due to the gas flow in the absence of mechanical agitation from the log-log plots. This procedure uses the  $k_L a$  value obtained for the 0 rpm. run and the  $k_L a$ 's for the 250 and 600 rpm. runs, other conditions being constant. The procedure was to connect the 250 and 600 rpm. points with a straight line and extend this line to the lower  $N^3 D^2$  values. Then a horizontal line corresponding to the  $k_L a$  value at 0 rpm. was drawn and made to intersect with the previously drawn line (see Figure 11). The  $N^3 D^2$  value corresponding to this point of intersection was then considered to be the agitation rate due to the gas flowing through the water. This intersection point, also encountered in the transition region, moved toward higher agitation rates for increasing superficial gas velocities. These points, as was the case before, also fell around a straight line with a rather high positive slope. This behavior indicates that as the gas flow rate is increased the agitation due to the gas flow is also increased. This was also noticed by others (9, 37) and correlated with the following equation by Calderbank and Moo-Young (9):

$$P/V = \rho V_s g/g_c \quad \text{IV-5}$$

It will be pointed out that the ratio of the slopes of the lines obtained from the transition region and air agitation points (Figure 11) may be an indication of the air agitation effect in the transition region. The remainder of the agitation is due to mechanical agitation. This is proposed because of the fact that in most sets of data the slope of the transition region line is larger than the slope of the air agitation line (Figure 11). The same phenomena can also be deduced from Karwat's (37) data.

Furthermore, the results of Hixson and Gaden (33), at 25°C, for air

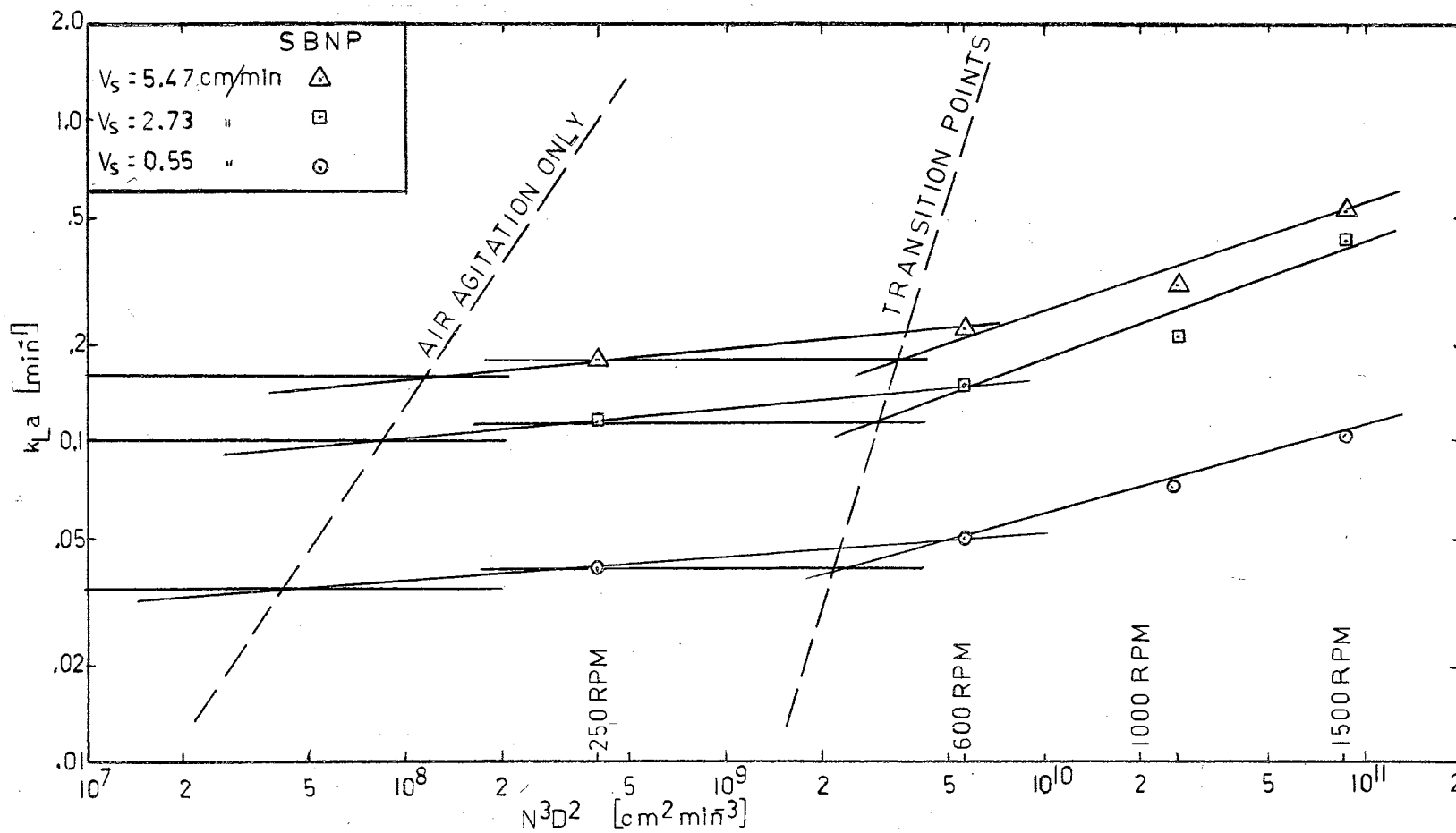


FIGURE II. COMPARISON BETWEEN THE DEPENDENCIES OF THE AIR AGITATION AND THE TRANSITION POINTS ON  $V_s$ ;  $T=10^\circ\text{C}$

agitation only are compared with the present data in Figure 12, as well as the results of Yoshida and Miura (77). This figure (i.e. Figure 12) covers a rather wide range of  $V_s$ 's and shows a favorable comparison among the three works.

$k_L a$  as a Function of  $N^3 D^2$ ,  $V_s$ , and T

When the different treatments of the previous parts are all combined, the following equation is obtained:

$$k_L a = C(N^3 D^2)^{0.37} (V_s)^{0.67} (T)^{0.34} \quad \text{IV-6}$$

This equation is similar to ones developed for similar systems. The equations reported previously did not include the influence of temperature, but some included other system variables, such as the geometry of the vessel, liquid height, etc., which were constant in this case. This relationship, like its successors, holds only for the higher  $N^3 D^2$  region, (i.e., to the right of the transition point in Figure 2), and in the region where the superficial gas velocity still has an effect.

The exponents were calculated for each case, and can be found in the appendices. The multiplying coefficient was found by using the average values of the exponents and by calculating back from the experimental  $k_L a$  data. Three values for this coefficient are given below:

$$C_{AL} = 6 \times 10^{-6} (\text{cm.}^{1.41} \text{ } \circ\text{C}^{0.34} / \text{min.}^{0.78}) \text{ average for all bubble sizes}$$

$$C_{SB} = 5 \times 10^{-6} (\text{cm.}^{1.41} \text{ } \circ\text{C}^{0.34} / \text{min.}^{0.78}) \text{ average for small bubbles}$$

$$C_{LB} = 7 \times 10^{-6} (\text{cm.}^{1.41} \text{ } \circ\text{C}^{0.34} / \text{min.}^{0.78}) \text{ average for large bubbles}$$

All calculated values are given in Appendix K.

Furthermore, in an attempt to describe the  $k_L a$  behavior in the

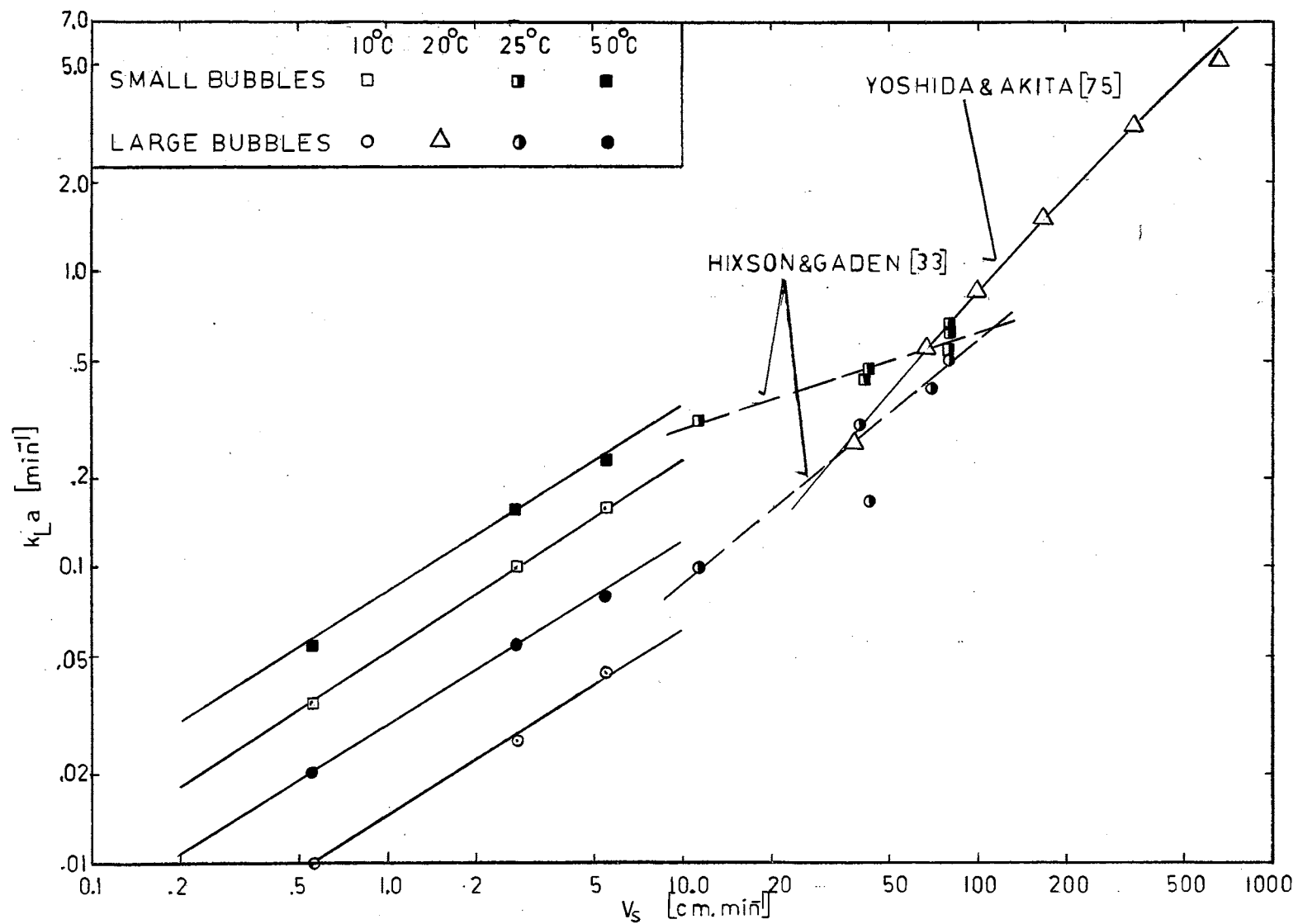


FIGURE 12. DEPENDENCY OF  $k_{La}$  ON  $V_s$  WITH NO MECHANICAL AGITATION

region of low agitation (predominantly gas agitation) with the calculated values of the exponents and the multiplying coefficient the following equation is proposed:

$$k_L a = \begin{cases} C_{AL} \\ C_{SB} \\ C_{LB} \end{cases} (N^3 D^2)_M^{0.37} (V_S)^{0.67} (T)^{0.34} \quad \text{IV-7}$$

Details on this equation are in Appendix J. The only thing different in this equation from Equation IV-6 is the fact that the  $(N^3 D^2)_M$  is not the real  $N^3 D^2$ , but a modified one.

The equations proposed above, one for each side of the transition region were used to back-calculate the  $k_L a$  values. Considering the amount of the generalizations made and also the scatter of data encountered in the literature, the calculated  $k_L a$  values were reasonable. In fact some of them agreed very closely with the experimental values. A table of comparison among these values is presented in Appendix L.

#### Sources of Experimental Error

Besides human errors that were introduced, experimental errors resulted from the various measuring apparatus and water used.

Experiments were run with tap water which was filtered through a bed of fine ion-exchange resin particles. Thus, the amount of impurities in the water may well have been an undetermined variable. This naturally would affect both the  $k_L$ , and the transfer area.

The stirrer speed was maintained as constant as possible. Its speed was frequently measured and, if necessary, was corrected during the run. For this reason a maximum of of 10% deviation in this variable could be expected. (This figure is based on the readings taken during

the experimental runs.)

The gas flow measurements were probably another source of error, since there was a time lag (approximately 5 - 10 seconds) between the time at which the valve was opened and the time at which the correct rotameter reading was achieved. Furthermore, during the adjustments the desired rotameter reading was sometimes over-shot, although this was immediately corrected by adjusting the valve setting.

The effect of the temperature on the experimental error is believed to be the smallest of all since the bath temperature was quite adequately controlled ( $\pm 0.5^{\circ}\text{C}$ ).

Another source of error might have been due to the oxygen analyzer. Although it is claimed to be "accurate"\* by the manufacturer, it had some uncertainties due to the shifting of the indicator needle and the minute amount of oxygen used up during the reaction. As can be seen from the data in Appendix C, the shifting of the indicator needle during a reading was found to have negligible influence on the taking of correct and reproducible readings.

Finally, another error was due to the  $k_L a$  determination from the raw data. The plots of time versus the logarithm of the ratios of the concentration differences were not absolutely straight lines in all of the runs, although they were approximated by straight lines.

---

\* Claimed to be "accurate within  $\pm 1\%$  of the reading, at constant temperature, in the range from 50 mm. of oxygen to 1000 mm. of oxygen" (3).

## CHAPTER V

### CONCLUSIONS AND RECOMMENDATIONS

This study includes (1) an introduction to the subject of gas-liquid mass transfer and the statement of the problem under study, (2) a literature survey, (3) an explanation of the experimental apparatus and (4) a discussion of the results obtained and their comparison with the results of the previous workers. Data, sample calculations, and the results of all the calculations performed for this work are given in the appendices.

Having discussed the results obtained from this work in some detail, and also compared them with other results, the following conclusions can be drawn for the range of system and operating conditions pertaining to this study:

1.  $k_L a$  can be correlated as a function of agitation rate, superficial gas velocity, and temperature:

$$k_L a = \left\{ \begin{array}{l} C_{AL} \\ C_{SB} \\ C_{LB} \end{array} \right\} (N^3 D^2)^{0.37} (V_s)^{0.67} (T)^{0.34}$$

2. Solid particles added to the contents of the agitated gas-liquid contactor (other things being constant) do not affect the  $k_L a$  values.
3. The transition point between the gas agitation and mechanical agitation regimes is probably a function of  $V_s$ , but more data

- is needed to test this point.
4. Agitation rate at no mechanical agitation is a function of the superficial gas velocity.
  5. With no mechanical agitation and at low  $V_s$ 's (the range of this work), the dependency of  $k_L a$  on  $V_s$  is the same as it is with mixing (see Figure 12).
  6. Surface aeration makes a very small contribution to the aeration rate under conditions covered in these experiments.
  7. At high agitation rates the bubbles from a larger sparger give the same  $k_L a$  values as the bubbles from a fine bubble sparger. This is due to the fact that at high agitation the large bubbles are broken into bubbles of the size of the bubbles produced by the fine bubble sparger.
  8. The slope of the  $k_L a$  versus stirrer speed plot for the lowest gas flow rate was different than the slopes of the lines for the other flow rates. This may mean that the recommendation of Westerterp, et al. (72) that the slopes of these plots are independent of the superficial gas velocity is not valid for very low flow rates.
  9. The  $\log k_L a$  versus  $\log N^3 D^2$  and similar plots did not show a straight line relationship in all cases as proposed by the previous workers (12, 25, 76, 77, etc.).
  10. From the results of the previous works and also from the results of this work it can be said that the exponent of the agitation rate is a function of the impeller, and also that this exponent is more dependent on the operating conditions than is the exponent of  $V_s$ .



11. The fact that the straight line that fits the transition points has a higher slope than the straight line that fits the air agitation points (Figure 11) may be an indication to the degree of gas agitation at low agitation rates, as well as the transition point.

This study and the above conclusions suggest the following recommendations for further work:

1. More accurate as well as other types of apparatus (torque dynamometer, different kinds of impellers, a motor with a steadier speed, different spargers, different sized tanks, etc.) should be procured. This will enable closer control of the variables, a larger range in the variables, and the measurement of additional important variables, such as power input, bubble size, gas hold-up, etc.
2. Use more than one sparger in a tank to determine the optimum number and location of the spargers. The optimum ratio of the gas rates from these spargers could also be studied.
3. Studies using more than one impeller, possibly in opposite directions, and also possibly placed at different positions in the agitated vessel would be useful.
4. More data should be taken to study the air-agitation only and transition regions.
5. The effect of the solid particles on  $k_L a$  should be studied under conditions different than those in this work. Possibly different specific gravities, sizes, shapes and numbers may be tried. Different impeller designs may also be studied in conjunction with the effect of the particles.

#### A SELECTED BIBLIOGRAPHY

1. Bartholomew, W. H., E. O. Karow, and M. R. Sfat. Ind. Eng. Chem., 42 (1950), 1801.
2. Becker, H. G. Ind. Eng. Chem., 16 (1924), 1220.
3. Beckman Instruments, Inc. "Beckman Instructions 1196.", Beckman Instruments, Inc., Fullerton, California, 1962.
4. Beckman Instruments, Inc., "Bulletin 7015A.", Beckman Instruments Inc., Fullerton, California, 1963.
5. Calderbank, P. H. Brit. Chem. Eng., 1 (1956), 206.
6. Calderbank, P. H. Trans. Inst. Chem. Eng. (London), 36 (1958), 443.
7. Calderbank, P. H. Trans. Inst. Chem. Eng. (London), 37 (1959), 173.
8. Calderbank, P. H., and A. C. Lochiel. Chem. Eng. Sci., 19 (1964), 485.
9. Calderbank, P. H., and M. B. Moo-Young. "The Proceedings of the International Symposium on Distillation," (1960), 59.
10. Carver, C. E. "Biological Treatment of Sewage and Industrial Wastes," Vol. 1. B. J. McCabe and W. W. Eckenfelder, Jr., Ed. New York: Reinhold Publishing Co., 1956.
11. Chiang, S. H., and H. L. Toor. A.I.Ch.E. Journal, 5 (1959), 165.
12. Cooper, C. M., G. A. Fernstrom, and S. A. Miller. Ind. Eng. Chem., 36 (1944), 504.
13. Danckwerts, P. V. Ind. Eng. Chem., 43 (1951), 1460.
14. Davies, J. T. "Advances in Chemical Engineering," Vol. 4. T. B. Drew, J. W. Hoopes, Jr., and T. Vermeulen, Ed. New York: Academic Press, 1963.
15. Davies, J. T., A. A. Kilmer, and G. A. Ratcliff. Chem. Eng. Sci., 19 (1964), 123.
16. Dienderfer, F. H., and A. E. Humphrey. Ind. Eng. Chem., 53 (1961), 755.
17. Dixon, B. E., and A. A. W. Russel. J. Soc. Chem. Ind. (London),

- 69 (1950), 284.
18. Dixon, B. E., and J. E. L. Swallow. J. App. Chem., 4 (1954), 86.
  19. Eckenfelder, W. W., Jr. Proc. Amer. Soc. Civ. Eng., SA4 (1959), 89.
  20. Eckenfelder, W. W., Jr., and E. L. Barnhart. A.I.Ch.E. Journal, 7 (1961), 631.
  21. Elsworth, R., V. Williams, and R. Harris-Smith. J. App. Chem., 7 (1957), 261.
  22. Fair, J. R., A. J. Lambright, and J. W. Andersen. Ind. Eng. Chem., Proc. Des. Dev., 1 (1962), 33.
  23. Frank-Kamenetskii, D. A. "Diffusion and Heat Exchange in Chemical Kinetics." New Jersey: Princeton University Press, 1955.
  24. Foust, H. C., D. E. Mack, and J. H. Rushton. Ind. Eng. Chem., 36 (1944), 517.
  25. Friedman, A. M., and E. N. Lightfoot, Jr. Ind. Eng. Chem., 49 (1957), 1227.
  26. Gal-or, B., and W. Resnick. Chem. Eng. Sci., 19 (1964), 653.
  27. Gal-or, B., and W. Resnick. "Gas Residence Time in Agitated Gas-Liquid Contactors, - Experimental Test of Mass-Transfer Model." To be published.
  28. Haberman, W. L., and R. K. Morton. Trans. Amer. Soc. Civ. Engrs., 121 (1956), 227.
  29. Hammerton, D., and F. H. Garner. Trans. Inst. Chem. Eng. (London), 32 (1954), 518.
  30. Hanhart, J., H. Kramers, and K. R. Westerterp. Chem. Eng. Sci., 18 (1963), 503.
  31. Higbie, R. Trans. Am. Inst. Chem. Eng., 31 (1935), 365.
  32. Himmelblau, E. M. Chem. Rev., 64 (1964), 527.
  33. Hixson, A. W., and E. L. Gaden, Ind. Eng. Chem., 42 (1950), 1792.
  34. Hyman, D., and J. M. Van Den Bogaerde. Ind. Eng. Chem., 52 (1960), 751.
  35. Hyman, D. "Advances in Chemical Engineering," Vol. 3. T. B. Drew, J. W. Hoopes, Jr., and T. Vermeulen, Ed. New York: Academic Press, 1962.
  36. Johnson, D. L., H. Saito, J. D. Polejes, and D. A. Hougen. A.I.Ch.E.

Journal, 3 (1957), 411.

37. Karwat, H. Chem. Ing. Tech. 31 (1959), 588.
38. Krenkel, P. A., and G. T. Orlob. Proc. Amer. Soc. Civ. Eng., SA2 (1962), 3079.
39. Leibson, I., E. G. Holcomb, A. G. Cacosso, and J. J. Jacnic. A.I.Ch.E. Journal, 2 (1956), 296.
40. Lewis, W. K., and W. G. Whitman. Ind. Eng. Chem., 16 (1924), 1215.
41. Levich, V. G. "Physico-Chemical Hydrodynamics." New Jersey: Prentice-Hall, Inc., 1962.
42. Licht, W., and J. B. Conway. Ind. Eng. Chem., 42 (1950), 1151.
43. Licht, W., and W. F. Pansing. Ind. Eng. Chem., 45 (1953), 1885.
44. Maxon, W. D., and M. J. Johnson. Ind. Eng. Chem., 45 (1953), 2555.
45. Michel, B. J., and S. A. Miller. A.I.Ch.E. Journal, 8 (1962), 262.
46. Miller, D. N. Ind. Eng. Chem., 56 (1964), 18.
47. Miyamoto, S. Bul. Chem. Soc. Jap., 5 (1930), 123.
48. Miyamoto, S. Bul. Chem. Soc. Jap., 7 (1932), 8.
49. Miyamoto, S., and T. Kaya. Bul. Chem. Soc. Jap., 5 (1930), 229.
50. Oldshue, J. Y. Ind. Eng. Chem., 48 (1956), 2194.
51. Olney, R. B. A.I.Ch.E. Journal, 7 (1961), 348.
52. Pasveer, A. Sew. Ind. Wastes, 25 (1953), 1253.
53. Pasveer, A. Sew. Ind. Wastes, 27 (1955), 1130.
54. Phillips, D. H., and M. J. Johnson. Ind. Eng. Chem., 51 (1959), 83.
55. Polejes, J. D., Ph.D. thesis, University of Wisconsin, 1959. (As referred to by 72).
56. Popovich, A. T., R. E. Jervis, and O. Trass. Chem. Eng. Sci., 19 (1964), 357.
57. Preen, B. V., Ph.D. thesis, University of Durham, South Africa, 1961. (As referred to in 72)
58. Quigley, C. J., A. I. Johnson, and B. L. Harris. Chem. Eng. Prog. Sym. Series, No. 16, 51 (1955), 31.

59. Rushton, J. H., J. B. Gallagher, and J. Y. Oldshue. Chem. Eng. Prog., 52 (1956), 319.
60. Schultz, J. S., and E. L. Gaden, Jr. Ind. Eng. Chem., 48 (1956), 2209.
61. Shulman, H. L., and M. C. Molstad. Ind. Eng. Chem., 42 (1950), 1058.
62. Snyder, J. R., P. F. Hagerty, and M. C. Molstad. Ind. Eng. Chem., 49 (1957), 689.
63. "Standard Methods for the Examination of Water, Sewage, and Industrial Wastes." Published jointly by American Public Health Association, American Water Works Association, and Federation of Sewage and Industrial Water Association, 10<sup>th</sup> Edition, New York, 1955.
64. Stefan, J. "Sitzungsberichte der Mathematisch-Naturwissenschaftlichen Classe der Kaiserlichen Akademie der Wissenschaften," Vienna, 77 (1878), 371; and 79 (1879), 161.
65. Toor, H. L., and J. M. Marchello. A.I.Ch.E. Journal, 4 (1958), 97.
66. Van De Vusse, J. G. Chem. Eng. Sci., 17 (1962), 507.
67. Van Krevelen, D. W., and P. H. Hoftijzer. Chem. Eng. Prog., 46 (1950) 29.
68. Vermeulen, T., G. M. Williams, and G. E. Langlois. Chem. Eng. Prog., 51 (1955), 85-F.
69. West, F. B., W. D. Gilbert, and T. Shimizu. Ind. Eng. Chem., 44 (1952), 2470.
70. Westerterp, K. R. Chem. Eng. Sci., 18 (1963), 495.
71. Westerterp, K. R. Chem. Eng. Sci., 19 (1964), 514.
72. Westerterp, K. R., L. L. Van Dierendonck, and J. A. de Kraa. Chem. Eng. Sci., 18 (1963), 157.
73. Whitman, W. G. Chem. Met. Eng., 29 (1923), 146.
74. Whitman, W. G., L. L. Long, and H. Y. Wang. Ind. Eng. Chem., 18 (1926), 363.
75. Yoshida, F., and K. Akita. A.I.Ch.E. Journal, 11 (1965), 9.
76. Yoshida, F., A. Ikeda, S. Imakawa, and Y. Miura. Ind. Eng. Chem., 52 (1960), 435.
77. Yoshida, F., and Y. Miura. Ind. Eng. Chem., Proc. Des. Dev., 2 (1963), 263.

**APPENDICES**

APPENDIX A

DISSOLVED OXYGEN ANALYZER CALIBRATION CHART

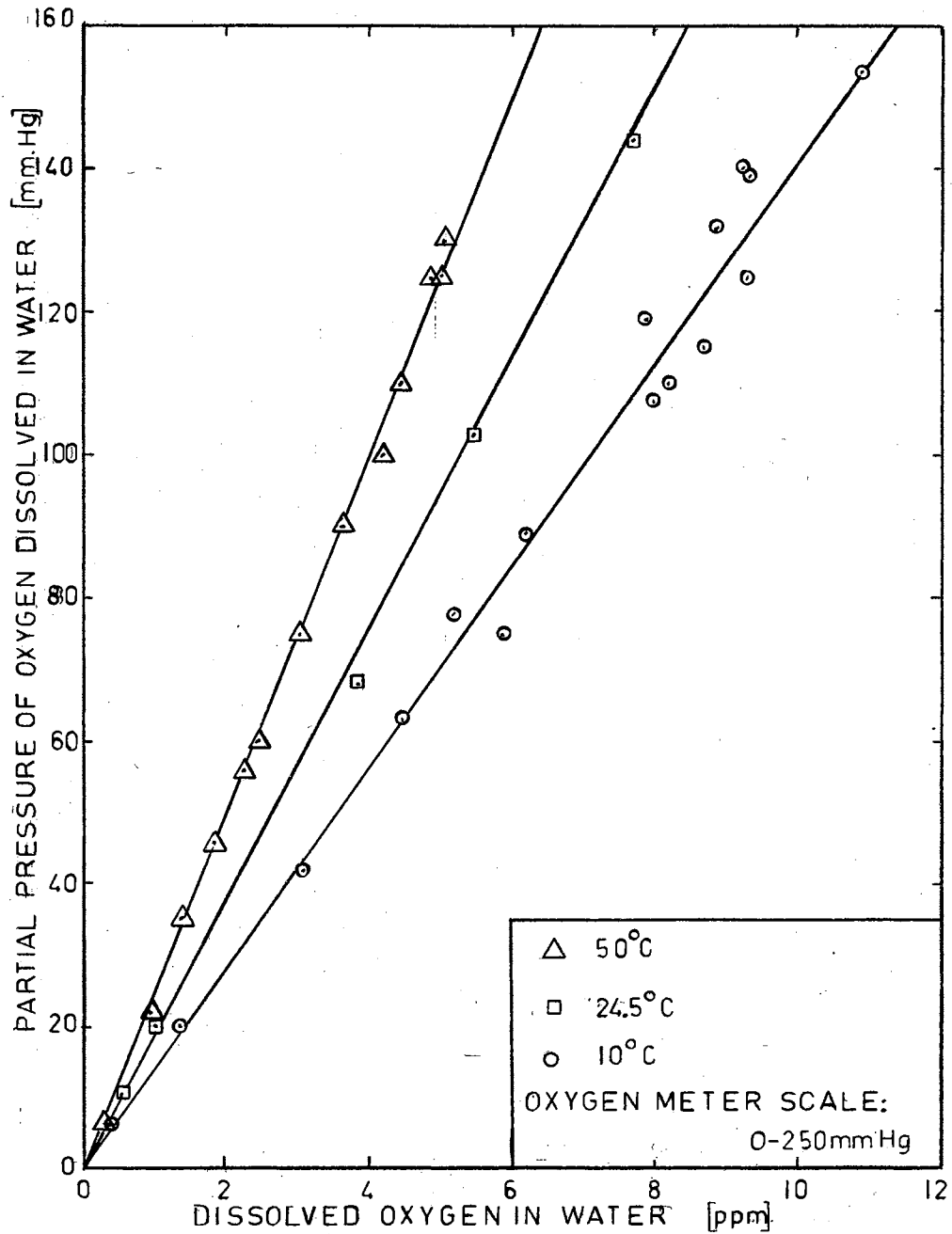


FIGURE 13. DISSOLVED OXYGEN ANALYZER CALIBRATION CHART

APPENDIX B

SAMPLE CHART AND CALCULATIONS FOR  $k_L a$  DETERMINATION

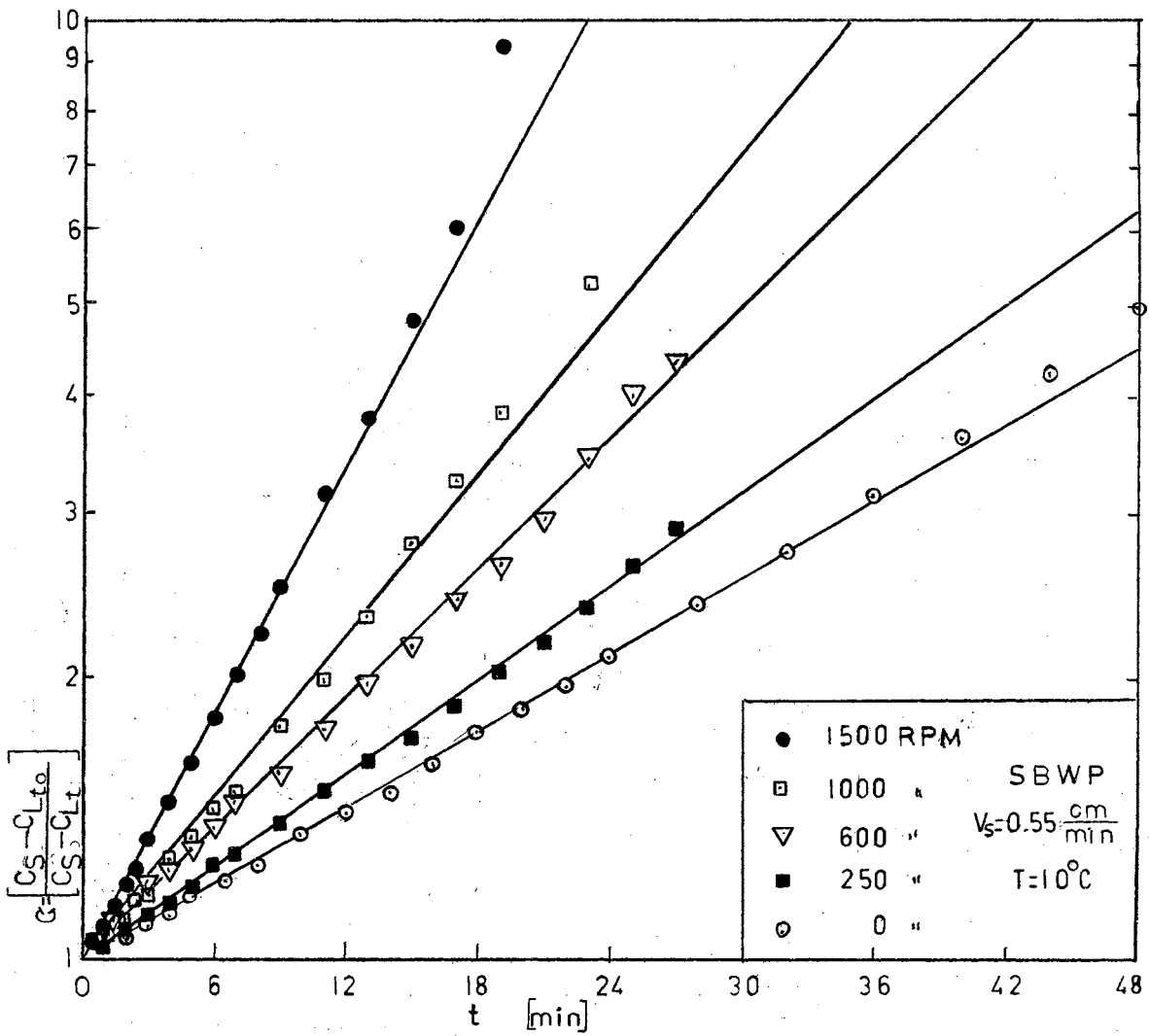


FIGURE 14. RAW DATA PLOT FOR  $k_L a$  DETERMINATION



## Sample Calculations:

RPM	N:	0	250	600	1000	1500
$\Delta t = t_2 - t_1$		48-13	36-20	31-13	25-14	21-9
$\Delta C = C_{t_2} - C_{t_1}$		4.50/1.50	4.00/2.15	5.20/2.00	5.20/2.50	8.50/2.50
$k_L a = \ln(\Delta C / \Delta t)$		0.0314	0.0388	0.0531	0.0666	0.1020

## APPENDIX C

### REPRODUCIBILITY OF THE $k_L a$ 's AND THE CONSISTENCY OF THE DISSOLVED OXYGEN ANALYZER READINGS

The average experimental deviation of the  $k_L a$  values was found to be 3.2%. This value was calculated from the data of runs made under similar conditions. The calculations that led to the above deviation were as follows:

1) SBNP;  $V_s = 0.55$  cm./min.;  $10^\circ\text{C}$ ; 0 RPM

$$\begin{array}{lll}
 k_L a(1) = 0.0348 \text{ min.}^{-1} & & \\
 k_L a(2) = 0.0331 \text{ min.}^{-1} & k_L a(\text{avg.}) = 0.0340 \text{ min.}^{-1} & \text{Dev.} = 2.65\%
 \end{array}$$

2) SBNP;  $V_s = 5.47$  cm./min.;  $10^\circ\text{C}$ ; 1500 RPM

$$\begin{array}{lll}
 k_L a(1) = 0.529 \text{ min.}^{-1} & & \\
 k_L a(2) = 0.571 \text{ min.}^{-1} & k_L a(\text{avg.}) = 0.550 \text{ min.}^{-1} & \text{Dev.} = 3.82\%
 \end{array}$$

3) SBWP;  $V_s = 2.73$  cm./min.;  $10^\circ\text{C}$ ; 1500 RPM

$$\begin{array}{lll}
 k_L a(1) = 0.392 \text{ min.}^{-1} & & \\
 k_L a(2) = 0.392 \text{ min.}^{-1} & k_L a(\text{avg.}) = 0.392 \text{ min.}^{-1} & \text{Dev.} = 0.00\%
 \end{array}$$

4) LBNP;  $V_s = 0.55$  cm./min.;  $10^\circ\text{C}$ ; 250 RPM

$$\begin{array}{lll}
 k_L a(1) = 0.0240 \text{ min.}^{-1} & & \\
 k_L a(2) = 0.0202 \text{ min.}^{-1} & k_L a(\text{avg.}) = 0.0221 \text{ min.}^{-1} & \text{Dev.} = 9.40\%
 \end{array}$$

5) LBNP;  $V_s = 0.55$  cm./min.;  $10^\circ\text{C}$ ; 600 RPM

$$\begin{array}{lll}
 k_L a(1) = 0.0264 \text{ min.}^{-1} & & \\
 k_L a(2) = 0.0228 \text{ min.}^{-1} & k_L a(\text{avg.}) = 0.0246 \text{ min.}^{-1} & \text{Dev.} = 7.96\%
 \end{array}$$

6) LBWP;  $V_s = 0.55$  cm./min.;  $10^\circ\text{C}$ ; 600 RPM

$$k_{L,a}(1) = 0.0229 \text{ min.}^{-1} \quad k_{L,a}(\text{avg.}) = 0.0240 \text{ min.}^{-1} \quad \text{Dev.} = 4.58\%$$

$$k_{L,a}(2) = 0.0250 \text{ min.}^{-1}$$

7) SBNP;  $V_s = 2.73$  cm./min.;  $50^\circ\text{C}$ ; 1000 RPM

$$k_{L,a}(1) = 0.353 \text{ min.}^{-1} \quad k_{L,a}(\text{avg.}) = 0.348 \text{ min.}^{-1} \quad \text{Dev.} = 1.72\%$$

$$k_{L,a}(2) = 0.342 \text{ min.}^{-1}$$

8) SBNP;  $V_s = 5.47$  cm./min.;  $50^\circ\text{C}$ ; 1000 RPM

$$k_{L,a}(1) = 0.523 \text{ min.}^{-1} \quad k_{L,a}(\text{avg.}) = 0.526 \text{ min.}^{-1} \quad \text{Dev.} = 0.68\%$$

$$k_{L,a}(2) = 0.530 \text{ min.}^{-1}$$

9) LBWP;  $V_s = 0.55$  cm./min.;  $10^\circ\text{C}$ ; 250 RPM

$$k_{L,a}(1) = 0.0216 \text{ min.}^{-1} \quad k_{L,a}(\text{avg.}) = 0.0207 \text{ min.}^{-1} \quad \text{Dev.} = 4.35\%$$

$$k_{L,a}(2) = 0.0198 \text{ min.}^{-1}$$

10) LBWP;  $V_s = 2.73$  cm./min.;  $10^\circ\text{C}$ ; 1500 RPM

$$k_{L,a}(1) = 0.2683 \text{ min.}^{-1} \quad k_{L,a}(\text{avg.}) = 0.2683 \text{ min.}^{-1} \quad \text{Dev.} = 0.00\%$$

$$k_{L,a}(2) = 0.2683 \text{ min.}^{-1}$$

11) LBWP;  $V_s = 5.47$  cm./min.;  $10^\circ\text{C}$ ; 0 RPM

$$k_{L,a}(1) = 0.2534 \text{ min.}^{-1} \quad k_{L,a}(\text{avg.}) = 0.2534 \text{ min.}^{-1} \quad \text{Dev.} = 0.00\%$$

$$k_{L,a}(2) = 0.2534 \text{ min.}^{-1}$$

---

Avg. Dev. = 3.19%

The consistency of the dissolved oxygen analyzer readings were determined in the following way: Water at constant temperature was put into the vessel and four consecutive readings were made by the oxygen analyzer in a period of approximately 2.5 minutes. This was followed by a 12 minute interval during which no readings were made and the water was not disturbed. Following this four more readings, again in approximately 2.5 minutes, were made and this also was followed by an

equally long interval (12 minutes) of rest, etc. For the purposes of covering a rather wide range of the oxygen concentration the above mentioned experiment was done with three different water samples at three different dissolved oxygen concentrations. The results are given below; the readings are in millimeters of mercury, i.e., partial pressure of dissolved oxygen, as read from the meter:

Temperature:	17.8°C	17.8°C	20.0°C
A-1	60.0	20.5	128.0
A-2	60.0	21.5	127.0
A-3	60.0	21.0	128.0
A-4	59.0	21.5	129.0
12 minutes			
B-1	62.0	26.0	130.5
B-2	62.0	25.5	130.0
B-3	61.5	26.0	130.5
B-4	61.0	25.0	130.5
12 minutes			
C-1	65.5	30.5	130.5
C-2	65.5	30.0	131.5
C-3	66.0	30.0	131.5
C-4	65.0	30.0	131.5
12 minutes			
D-1	70.0	35.5	133.0
D-2	70.5	35.5	133.0
D-3	70.0	35.5	133.5
D-4	70.5	36.0	134.0

APPENDIX D

EXPERIMENTAL  $k_L a$  VALUES

RPM	0	250	600	1000	1500
<u>SBNP; 10°C:</u>					
$V_s = 0.55$ cm./min.	0.0348	0.0405	0.0502	0.0725	0.1068
$V_s = 2.73$ cm./min.	0.1015	0.1173	0.1509	0.2175	0.4233
$V_s = 5.47$ cm./min.	0.1590	0.1810	0.2242	0.3101	0.5291
<u>SBWP; 10°C:</u>					
$V_s = 0.55$ cm./min.	0.0314	0.0388	0.0531	0.0666	0.1020
$V_s = 2.73$ cm./min.	0.0930	0.1183	0.1575	0.2168	0.3920
$V_s = 5.47$ cm./min.	0.1551	0.1760	0.2075	0.3008	0.5435
<u>LBNP; 10°C:</u>					
$V_s = 0.55$ cm./min.	0.0099	0.0240	0.0264	0.0567	0.0926
$V_s = 2.73$ cm./min.	0.0267	0.0447	0.0958	0.1679	0.2968
$V_s = 5.47$ cm./min.	0.0455	0.0794	0.1413	0.2830	0.4621
<u>LBWP; 10°C:</u>					
$V_s = 0.55$ cm./min.	0.0099	0.0216	0.0250	0.0560	0.0926
$V_s = 2.73$ cm./min.	0.0311	0.0573	0.0909	0.1532	0.2683
$V_s = 5.47$ cm./min.	0.0446	0.0632	0.1010	0.2534	0.4605
<u>LBNP; 50°C:</u>					
$V_s = 0.55$ cm./min.	0.0209	0.0337	0.0480	0.1027	0.1582
$V_s = 2.73$ cm./min.	0.0543	0.0870	0.1718	0.3141	0.5477
$V_s = 5.47$ cm. min.	0.0805	0.1197	0.2215	0.4270	0.7668

## APPENDIX D (continued)

SBNP; 50°C:

$V_s = 0.55$ cm./min.	0.0554	0.0798	0.0968	0.1326	0.1780
$V_s = 2.73$ cm./min.	0.1537	0.1938	0.2488	0.3424	0.5905
$V_s = 5.47$ cm./min.	0.2313	0.3062	0.4193	0.5297	0.9041

## APPENDIX E

### BUBBLE SIZES

As mentioned in Chapter III, the bubble sizes were determined by a comparative method, i.e., by submerging an object of known size into the agitated vessel as the air was bubbled through the liquid and the vessel operated under conditions similar to the conditions of the experimental runs. These measurements were made at the ambient temperature (approximately 25°C), since the agitated vessel had to be taken out of the constant temperature bath for visual comparison of the bubble sizes with the size of the submerged object. The results were:

#### Small Bubble Sparger:

$V_s$	RPM	Bubble Size	Comments
0.55 cm./min.	0	<0.1-0.3 cm.	spheres, rather uniform shape and size
5.47 cm./min.	0	0.1-0.3 cm.	" " " " " "
0.55 cm./min.	1000	0.1-0.3 cm.	" " " " " "
5.47 cm./min.	1000	0.1-0.3 cm.	" " " " " "

#### Large Bubble Sparger:

$V_s$	RPM	Bubble Sizes	Comments
0.55 cm./min.	0	0.3-0.5 cm.	spheres, ellipsoids
5.47 cm./min.	0	0.4-0.8-1.0 cm.	ellipsoids, spherical caps, non-uniform shapes and sizes
0.55 cm./min.	1000	0.1-0.3 cm.	spheres
5.47 cm./min.	1000	0.1-0.3 cm.	spheres

## APPENDIX F

### EFFECT OF SURFACE AERATION

The  $k_L a$  values at 24°C are given below for the surface aeration of the water in the agitated vessel at two stirrer speeds. These values are comparatively smaller than the corresponding  $k_L a$  values of the runs at 10 and 50°C, approximately equal stirrer speeds and at the lowest superficial gas velocity. From these values of  $k_L a$  it is seen that the effect of surface aeration compared with bubble aeration is appreciably small.

Temperature:	10°C	24°C	50°C
<u><math>V_s = 0.00</math> cm./min.:</u>			
900 RPM	-	0.00377 min. <sup>-1</sup>	-
1500 RPM	-	0.00619 min. <sup>-1</sup>	-
<u><math>V_s = 0.55</math> cm./min.:</u>			
1000 RPM (SBNP)	0.0725 min. <sup>-1</sup>	-	0.1326 min. <sup>-1</sup>
1500 RPM (SBNP)	0.1068 min. <sup>-1</sup>	-	0.1780 min. <sup>-1</sup>
1000 RPM (LBNP)	0.0567 min. <sup>-1</sup>	-	0.1027 min. <sup>-1</sup>
1500 RPM (LBNP)	0.0926 min. <sup>-1</sup>	-	0.1582 min. <sup>-1</sup>



APPENDIX G

EXPONENTS OF  $N^3D^2$ , AND  $N_{Re}$

The exponents of correlation variables were calculated by fitting a straight line through the data points on the related plots, i.e.,  $\log k_L a$  vs.  $\log N^3D^2$ , and  $\log k_L a$  vs.  $\log N_{Re}$ , for the higher agitation range. The average of these slopes was used as the exponent in the calculation of the  $k_L a$ 's from the correlation. These slopes are

Exponents of  $N^3D^2$ :

----- 10°C ----- 50°C -----

$V_s = 0.55$  cm./min.:

SBNP	0.27	LBNP	0.46	LBNP	0.44
SBWP	0.23	LBWP	0.48	SBNP	0.22

$V_s = 2.73$  cm./min.:

SBNP	0.37	LBNP	0.41	LBNP	0.42
SBWP	0.33	LBWP	0.39	SBNP	0.31

$V_s = 5.47$  cm./min.:

SBNP	0.31	LBNP	0.43	LBNP	0.45
SBWP	0.35	LBWP	0.55	SBNP	0.27

Average = 0.37

Average deviation = 22.1%

Exponents of  $N_{Re}$  :

----- 10°C ----- 50°C -----

 $V_s = 0.55$  cm./min.:

SBNP	0.82	LBNP	1.38	LBNP	1.31
SBWP	0.70	LBWP	1.44	SBNP	0.66

 $V_s = 2.73$  cm./min.:

SBNP	1.11	LBNP	1.23	LBNP	1.26
SBWP	0.98	LBWP	1.18	SBNP	0.93

 $V_s = 5.47$  cm./min.:

SBNP	0.92	LBNP	1.30	LBNP	1.35
SBWP	1.04	SBWP	1.66	SBNP	0.82

Average = 1.12

Average deviation = 20.9%

APPENDIX H

EXPONENTS OF  $V_s$

T(°C)	RPM:	0	250	600	1000	1500
10	SBNP	0.66	0.65	0.66	0.64	0.72
10	SBWP	0.69	0.66	0.61	0.67	0.75
10	LBNP	0.65	0.50	0.74	0.69	0.70
10	LBWP	0.66	0.49	0.64	0.65	0.69
50	LBNP	0.59	0.56	0.69	0.63	0.70
50	SBNP	0.62	0.58	0.63	0.60	0.71

Average of all = 0.65

Average deviation = 6.92%

Average of 600, 1000, and 1500 RPM runs = 0.67

Average deviation = 7.7%

APPENDIX I

EXPONENTS OF T

$V_s$ cm./min.	RPM:	0	250	600	1000	1500
0.55	SBNP	0.32	0.38	0.40	0.42	0.29
2.73	SBNP	0.26	0.31	0.31	0.28	0.21
5.47	SBNP	0.25	0.34	0.43	0.35	0.32
0.55	LBNP	0.46	0.21	0.36	0.37	0.32
2.73	LBNP	0.44	0.42	0.36	0.39	0.39
5.47	LBNP	0.35	0.25	0.28	0.26	0.32

Average of large bubble exponents = 0.35

Average of small bubble exponents = 0.32

Average of all = 0.34

Average deviation = 16.1%

## APPENDIX J

### $N^3D^2$ FOR THE GAS AGITATION REGION

If one assumes that the  $k_L a$ 's for the  $N^3D^2$  values below the transition point value fall on a horizontal line passing through the  $k_L a$  value at the transition point, then for this region the correlation could be written as

$$k_L a = C(N^3D^2)_x^m (V_s)^n (T)^p \quad (J-1)$$

where  $(N^3D^2)_x$  is the transition point agitation rate. As shown in Appendix L,  $k_L a$  values were calculated by the above mentioned correlation for the 250 RPM. In these calculations only one value was used for  $(N^3D^2)_x$ . This value was the average of all the transition points of the experiments. This kind of an assumption is by no means correct since  $(N^3D^2)_x$  could be correlated as a function of  $V_s$  if enough data were available. This point was discussed before.

In addition, two other expressions were used in an effort to bring the calculated  $k_L a$ 's nearer to the experimentally determined  $k_L a$ 's (see Appendix L for calculations). These two equations are:

$$(N^3D^2)_M^m = (N^3D^2)^m \frac{(N^3D^2)_x}{(N^3D^2)_o} - 1^m \quad (J-2)$$

and,

$$(N^3D^2)_M^m = (N^3D^2)^m \frac{(N^3D^2)_x}{(N^3D^2)} - 1^m \quad (J-3)$$

where  $(N^3D^2)_x$  and  $(N^3D^2)_o$  are respectively the average transition point and the average  $N^3D^2$  values with no mechanical agitation. As mentioned

before both of these, i.e.,  $(N^3 D^2)_x$ , and  $(N^3 D^2)_o$ , could be correlated as function of  $V_s$ .

APPENDIX K

VALUES OF THE CORRELATION CONSTANT

When the experimental  $k_L a$ ,  $V_s$ ,  $N^3 D^2$ , and T values, and the average values of the exponents were used, the values obtained for the

$$k_L a = C (N^3 D^2)^{0.37} (V_s)^{0.67} (T)^{0.34}$$

correlation constant were:

----- 10°C ----- 50°C -----

$V_s = 0.55$  cm./min.; 250 RPM:

SBNP	0.000018	LBNP	0.000011	LBNP	0.000009
SBWP	0.000017	LBWP	0.000009	SBNP	0.000021

$V_s = 2.73$  cm./min.; 250 RPM:

SBNP	0.000018	LBNP	0.000006	LBNP	0.000007
SBWP	0.000018	LBWP	0.000008	SBNP	0.000017

$V_s = 5.47$  cm./min.; 250 RPM:

SBNP	0.000017	LBNP	0.000007	LBNP	0.000006
SBWP	0.000017	LBWP	0.000006	SBNP	0.000017

$V_s = 0.55$  cm./min.; 600 RPM:

SBNP	0.000008	LBNP	0.000001	LBNP	0.000004
SBWP	0.000009	LBWP	0.000004	SBNP	0.000001

## APPENDIX K (continued)

$V_s = 2.73$  cm./min.; 600 RPM:

SBNP	0.000008	LBNP	0.000005	LBNP	0.000005
SBWP	0.000009	LBWP	0.000005	SBNP	0.000008

$V_s = 5.47$  cm./min.; 600 RPM:

SBNP	0.000008	LBNP	0.000005	LBNP	0.000004
SBWP	0.000007	LBWP	0.000003	SBNP	0.000009

$V_s = 0.55$  cm./min.; 1000 RPM:

SBNP	0.000016	LBNP	0.000005	LBNP	0.000005
SBWP	0.000006	LBWP	0.000005	SBNP	0.000007

$V_s = 2.73$  cm./min.; 1000 RPM:

SBNP	0.000007	LBNP	0.000005	LBNP	0.000006
SBWP	0.000007	LBWP	0.000005	SBNP	0.000006

$V_s = 5.47$  cm./min.; 1000 RPM:

SBNP	0.000006	LBNP	0.000005	LBNP	0.000005
SBWP	0.000006	LBWP	0.000005	SBNP	0.000006

$V_s = 0.55$  cm./min.; 1500 RPM:

SBNP	0.000006	LBNP	0.000005	LBNP	0.000005
SBWP	0.000006	LBWP	0.000005	SBNP	0.000006

$V_s = 2.73$  cm./min.; 1500 RPM:

SBNP	0.000009	LBNP	0.000006	LBNP	0.000006
SBWP	0.000008	LBWP	0.000005	SBNP	0.000007

$V_s = 5.47$  cm./min.; 1500 RPM:

SBNP	0.000007	LBNP	0.000006	LBNP	0.000000
SBWP	0.000007	LBWP	0.000006	SBNP	0.000000



## APPENDIX K (continued)

$$C_{AL} = 0.000006 (\text{cm}^{1.41} \circ C^{0.34} / \text{min}^{0.78}) \quad - \quad \text{Average for all bubbles}$$
$$C_{LB} = 0.000005 (\text{cm}^{1.41} \circ C^{0.34} / \text{min}^{0.78}) \quad - \quad \text{Average for large bubbles}$$
$$C_{SB} = 0.000007 (\text{cm}^{1.41} \circ C^{0.34} / \text{min}^{0.78}) \quad - \quad \text{Average for small bubbles}$$

APPENDIX L

COMPARISON OF THE EXPERIMENTAL AND CALCULATED  $k_L a$ 's

The calculated  $k_L a$  values given below were calculated several ways as indicated. The calculated  $k_L a$ 's for the 250 RPM cases are followed by either (J-1), (J-2), or (J-3) indicating that they were calculated by the  $(N^3 D^2)_M$  term as given in equations (J-1), (J-2), and (J-3) respectively.

RPM:	250	600	1000	1500
<u><math>V_s = 0.55</math> cm./min.; <math>10^\circ\text{C}</math>:</u>				
Data (SBNP)	0.0405	0.0502	0.0725	0.1068
Data (LBNP)	0.0241	0.0264	0.0567	0.0926
$C = C_{AL}$	0.0254 (J-1) 0.0271 (J-2) 0.0242 (J-3)	0.0390	0.0613	0.0961
$C = C_{SB}$	0.0298 (J-1) 0.0316 (J-2) 0.0282 (J-3)	0.0455	0.0715	0.1120
$C = C_{LB}$	0.0212 (J-1) 0.0226 (J-2) 0.0202 (J-3)	0.0323	0.0511	0.0800
<u><math>V_s = 2.73</math> cm./min.; <math>10^\circ\text{C}</math>:</u>				
Data (SBNP)	0.1173	0.1509	0.2175	0.4233
Data (LBNP)	0.0447	0.0958	0.1679	0.2968
$C = C_{AL}$	0.0385 (J-1) 0.0796 (J-2) 0.0706 (J-3)	0.1019	0.1802	0.2823

## APPENDIX L (continued)

$C = C_{SB}$	0.0449 (J-1)	0.1189	0.2120	0.3398
	0.0930 (J-2)			
	0.0825 (J-3)			

$C = C_{LB}$	0.0321 (J-1)	0.0850	0.1502	0.2354
	0.0664 (J-2)			
	0.0590 (J-3)			

$V_s = 5.47$  cm./min.;  $10^\circ\text{C}$ :

Data (SBNP)	0.1810	0.2242	0.3101	0.5291
-------------	--------	--------	--------	--------

Data (LBNP)	0.0794	0.1413	0.2830	0.4621
-------------	--------	--------	--------	--------

$C = C_{AL}$	0.0615 (J-1)	0.1622	0.2870	0.4500
	0.1268 (J-2)			
	0.1130 (J-3)			

$C = C_{SB}$	0.0719 (J-1)	0.1193	0.3350	0.5250
	0.1479 (J-2)			
	0.1318 (J-3)			

$C = C_{LB}$	0.0514 (J-1)	0.0854	0.2394	0.3747
	0.1057 (J-2)			
	0.0942 (J-3)			

$V_s = 0.55$  cm./min.;  $50^\circ\text{C}$ :

Data (SBNP)	0.0798	0.0968	0.1326	0.1780
-------------	--------	--------	--------	--------

Data (LBNP)	0.0337	0.0480	0.1027	0.1582
-------------	--------	--------	--------	--------

$C = C_{AL}$	0.0224 (J-1)	0.0589	0.1040	0.1592
	0.0460 (J-2)			
	0.0410 (J-3)			

$C = C_{SB}$	0.0261 (J-1)	0.0686	0.1214	0.1859
	0.0536 (J-2)			
	0.0479 (J-3)			

$C = C_{LB}$	0.0186 (J-1)	0.0490	0.0868	0.1328
	0.0383 (J-2)			
	0.0342 (J-3)			

$V_s = 2.73$  cm./min.;  $50^\circ\text{C}$ :

Data (SBNP)	0.1938	0.2488	0.3424	0.5905
-------------	--------	--------	--------	--------

Data (LBNP)	0.0870	0.1718	0.3141	0.5477
-------------	--------	--------	--------	--------

## APPENDIX L (continued)

$C = C_{AL}$	0.0654 (J-1)	0.1730	0.3060	0.5905
	0.1351 (J-2)			
	0.1200 (J-3)			
$C = C_{SB}$	0.0763 (J-1)	0.2017	0.3674	0.5600
	0.1580 (J-2)			
	0.1400 (J-3)			
$C = C_{LB}$	0.0545 (J-1)	0.1442	0.2554	0.4000
	0.1128 (J-2)			
	0.1000 (J-3)			
<u><math>V_s = 5.47 \text{ cm./min.}; 50^\circ\text{C}:</math></u>				
Data (SBNP)	0.3063	0.4193	0.5290	0.9042
Data (LBNP)	0.1197	0.2215	0.4270	0.7668
$C = C_{AL}$	0.1044 (J-1)	0.2755	0.4875	0.7643
	0.2152 (J-2)			
	0.1920 (J-3)			
$C = C_{SB}$	0.0725 (J-1)	0.2627	0.5690	0.8910
	0.2512 (J-2)			
	0.2240 (J-3)			
$C = C_{LB}$	0.0871 (J-1)	0.1449	0.4060	0.6360
	0.1793 (J-2)			
	0.1600 (J-3)			

## NOMENCLATURE

<u>Symbol</u>		<u>Dimension</u>
a	Specific interfacial area	1/L
C, C'	Correlation constants	changes
C <sub>AL</sub>	Correlation constant for all bubble sizes	changes
C <sub>LB</sub>	Correlation constant for large bubbles	changes
C <sub>SB</sub>	Correlation constant for small bubbles	changes
Q	Dimensionless concentration, $Q = \frac{C_S - C_{L_0}}{C_S - C_{L_t}}$	-
Q <sub>t<sub>1</sub></sub> , Q <sub>t<sub>2</sub></sub>	Dimensionless concentration at time 1, and time 2	-
C <sub>G</sub>	Concentration of oxygen in gas	M/L <sup>3</sup>
C <sub>L<sub>t</sub></sub>	Dissolved oxygen concentration in water at any time t	M/M
C <sub>o</sub> , C <sub>L<sub>o</sub></sub>	Initial oxygen concentration in water	M/M
D <sup>i</sup>	Impeller diameter (Tables)	L
D	Oxygen diffusivity in water	L <sup>2</sup> /θ
D <sub>B</sub>	Bubble diameter	L
D <sub>o</sub>	Orifice diameter	L
d	Impeller diameter	L
F	Mean rate of surface renewal	1/θ
g	Acceleration due to gravity	L <sup>2</sup> /θ
g <sub>c</sub>	Gravitational conversion factor	(M/F)(L/θ <sup>2</sup> )
k	Mass transfer coefficient	L/θ

$k_L$	Liquid side mass transfer coefficient	L/θ
$k_L a$	Volumetric mass transfer coefficient (mass transfer coefficient interfacial area product)	1/θ
m	Exponent of the mechanical agitation factor	-
N	Stirrer speed, RPM.	1/θ
n	Exponent of the superficial gas velocity factor	-
$N^3 D^2$	Power factor	$L^2/\theta^3$
$(N^3 D^2)_M$	Modified power factor	changes
$(N^3 D^2)_x$	Power factor at the transition point	$L^2/\theta^3$
$(N^3 D^2)_o$	Power factor at air agitation only	$L^2/\theta^3$
$N_{Re}$	Reynolds number, $N_{Re} = \frac{ND^2}{\nu}$	-
P	Power input	FL/θ
P/V	Power input per unit volume	F/θL <sup>2</sup>
t	Time	θ
$t_e$	Exposure time	θ
T	Temperature	T
T'	Tank diameter	L
u	Velocity in the boundary layer	L/T
$u_\infty$	Velocity at or outside the boundary layer	L/T
$u_o, u_o'$	Threshold velocities	L/T
$V_s$	Superficial gas velocity	L/T
Z	Liquid height	L

Greek Letters

$\delta$	Film thickness	L
$\rho$	Density	M/L <sup>3</sup>
$\mu$	Viscosity	M/Lθ

$\nu$	Kinematic viscosity	$L^2/\theta$
$\emptyset$	Gas holdup (%)	-

VITA

Öner Hortaçsu

Candidate for the Degree of  
Master of Science

Thesis: GAS-LIQUID MASS TRANSFER IN AN AGITATED VESSEL:  
AIR-WATER SYSTEM

Major Field: Chemical Engineering

Biographical:

Personal Data: Born in İzmir, Turkey, February 26, 1940, the son of Ali and Müşerref Hortaçsu.

Education: Attended primary school in İstanbul, Turkey; graduated from Robert Academy (Robert College), İstanbul, in 1956, and from Robert College (Lycee), in 1959; received the Bachelor of Science degree from Robert College in June, 1963; completed the requirements for the Master of Science degree in August, 1965.

Professional Experience: Employed as a Summer Engineering trainee with Mensucat Santral T.A.Ş. in İstanbul, Turkey in the summer of 1961, and also by Mobil-Oil Austria A.G. in Vienna, Austria in the summer of 1962.